School of Finance

University of St.Gallen

Are Correlations Constant? Empirical and Theoretical Results on Popular Correlation Models in Finance

Zeno Adams
Roland Füss
Thorsten Glück

Working Papers on Finance No. 2016/13

Swiss Institute of Banking and Finance (S/BF – HSG)

June 2016

Are Correlations Constant? Empirical and Theoretical Results on Popular Correlation Models in Finance*

Zeno Adams[‡], Roland Füss[†], Thorsten Glück[§]

Working Paper

This version: June 2016

* An earlier version of this paper circulated under the title “Spurious Dynamic Conditional Correlation”. We would like to thank Chris Brooks, Daniel Buncic, Matthias Fengler, Massimo Guidolin, Michael Massmann, Jan Mutl, Adrian Pagan, David Rapach, and the participants of the SEPS Seminar at the University of St.Gallen for valuable comments and suggestions.

‡ Swiss Institute of Banking and Finance (s/bf), University of St.Gallen, Rosenbergstrasse 52, 9000 St. Gallen, Switzerland, Phone: +41 (0)71 224 7057, Fax: +41 (0)71 224 7088, Email: zeno.adams@unisg.ch.

† Swiss Institute of Banking and Finance (s/bf), University of St.Gallen, Rosenbergstrasse 52, 9000 St. Gallen, Switzerland, and Research Associate at the Centre for European Economic Research (ZEW), Mannheim, Germany, Phone: +41 (0)71 224 7055, Fax: +41 (0)71 224 7088, Email: roland.fuess@unisg.ch.

§ d-fine GmbH, Opernplatz 2, 60313 Frankfurt am Main, Germany, Phone: +49 (0)69 907370, Email: info@d-fine.de.

Are Correlations Constant? Empirical and Theoretical Results on Popular Correlation Models in Finance

Abstract

Multivariate GARCH models have been designed as an extension of their univariate counterparts. Such a view is appealing from a modeling perspective but imposes correlation dynamics that are similar to time-varying volatility. In this paper, we argue that correlations are quite different in nature. We demonstrate that the highly unstable and erratic behavior that is typically observed for the correlation among financial assets is to a large extent a statistical artefact. We provide evidence that spurious correlation dynamics occur in response to financial events that are sufficiently large to cause a structural break in the time-series of correlations. A measure for the autocovariance structure of conditional correlations allows us to formally demonstrate that the volatility and the persistence of daily correlations are not primarily driven by financial news but by the level of the underlying true correlation. Our results indicate that a rolling-window sample correlation is often a better choice for empirical applications in finance.

Keywords: *Change-point tests; correlation breaks*; *dynamic conditional correlation (DCC); multivariate GARCH models; spurious conditional correlation.*

JEL-Classification: *C*12, *C*52, *G*01, *G*11

1 Introduction

Multivariate GARCH models have been designed as extensions of their univariate counterparts. Engle, Granger, and Kraft (1984) present an early version as “a bivariate generalization of Engle’s ARCH model”. This view is conceptually appealing and has found widespread use in practice. In this paper, we argue that the nature of dynamic correlations is very different from that of conditional volatilities. While important economic and financial news such as economic activity, interest rate changes, and oil prices affect the volatility of financial assets, the relevance and impact of this news is often similar across firms. As a consequence, volatility is constantly exposed to news and therefore time-varying by nature but correlation changes are only observable after major economic events. For instance, correlations substantially increased for many financial assets following the burst of the Dot-com bubble in 2001 or the default of Lehman Brothers in September 2008 (Ofek and Richardson, 2003; Wied, Krämer, and Dehling, 2012) but correlations are generally insensitive to changes in macroeconomic variables such as interest rates or inflation (King, Sentana, and Wadhwani, 1994; Karolyi and Stulz, 1996). We demonstrate how current conditional correlation models tend to impose purely artificial dynamics on estimated conditional correlations and show why in empirical applications the estimated parameters governing the dynamics are often statistically significant despite the fact that underlying correlations are constant.

The correlation matrix is the input to many applications in finance and several recent studies seem to believe in the importance of time-varying correlations. For instance, Moskowitz (2003) emphasizes the significance of dynamic conditional correlations during recessions and periods of financial distress. Similarly, Adrian and Brunnermeier (2016) argue that MGARCH models are important for capturing the dynamic evolution of systemic risk. DeMiquel, Garlappi, and Uppal (2009) claim that allowing for time-varying moments could increase the performance of optimal asset allocation. The notion of constant correlations therefore has important implications for financial modeling and practice. Under a constant correlation matrix, international asset portfolios may not have the same degree of diversification than comparable portfolios based on dynamic correlations, portfolio optimization could generate different weights, and risk measures may indicate different levels of risk. The aim of our research is not to dismiss dynamic correlation modeling altogether, but to provide a critical perspective on popular models that are routinely used to generate estimates of dynamic asset correlations.

The analysis in this paper is based on Engle's (2002) Dynamic Conditional Correlation (DCC) model. The main advantage of the DCC approach is its parsimonious specification which simplifies interpretation and allows even large asset portfolios to be estimated within seconds. Over the last years, the DCC model has therefore become well-established in both research and practice.[1] In Appendix A of this paper, we show that our results also hold for other popular MGARCH models, which tend to generate very similar dynamics.[2] To illustrate its behavior, consider the conditional correlations between the daily returns of the S&P 500 and the NASDAQ index from 1990 to 2014 shown in Figure 1. Two characteristics that are typical for conditional correlations generated by MGARCH models stand out. First, conditional correlations undergo large swings over a short period of time. In the 1990's,

[1] For instance, the DCC model has been used in value-at-risk estimation (Pérignon and Smith, 2010), the analysis of asset class comovements (You and Daigler, 2010; Heaney and Srinanthakumar, 2012), the implementation of hedging strategies (Chang, McAleer, and Tansuchat, 2011), and the examination of correlation responses to announcement effects (Brenner, Pasquariello, and Subrahmanyam, 2009), among others.

[2] Only models that have become accepted in practice and can be applied with reasonable effort and speed are part of our robustness section. This includes MGARCH models with autoregressive covariances such as the corrected DCC model of Aielli (2013), the diagonal VECH model of Bollerslev, Engle, and Wooldridge (1988), or the diagonal BEKK model of Engle and Kroner (1995). It excludes more complex MGARCH specification such as the regime-switching model of Pelletier (2006). For a classification of MGARCH models we refer the reader to Bauwens, Laurent, and Rombouts (2006).

correlations frequently moved within a wide range between 0.52 in July 1993 and 0.94 in November 1997. In the literature, this observation has been sometimes interpreted as evidence that the underlying correlation structure is a highly volatile process (e.g., Pukthuanthong and Roll, 2011; Sadorsky, 2012). Second, the fluctuation in conditional correlations often changes over time. In Figure 1, correlations are highly volatile during the 1990's but enter a more tranquil period in 2000. During this time, the daily volatility of correlations dropped approximately by half. In this paper, we show that the large fluctuations during the 1990's and the small fluctuations during the 2000's have no fundamental economic cause but are purely artificial results generated by the DCC model.

<< Figure 1 about here >>

We demonstrate that the volatility of estimated conditional correlations $\hat{\rho}$ is a negative function of the underlying true correlation level ρ: The fluctuations in conditional correlations $\hat{\rho}$ are large when the correlation level ρ is close to zero and small when ρ approaches ± 1. In Figure 1, this causes the volatility to decrease drastically as conditional correlations reach values of 0.9 and beyond. In fact, we argue that for financial assets, underlying true correlations ρ are generally constant and that the fluctuations generated by autoregressive-type multivariate GARCH models are spurious. They are caused by infrequent economic disruptions that shift the level of correlations. We recognize that correlations can and do change from time to time. For instance, Longin and Solnik (1995), Bera and Kim (2002), and Forbes and Rigobon (2002) show that correlations among financial assets increase during economic crises and times of financial distress. However, our claim is that these level shifts are a very different type of dynamics than the daily autoregressive fluctuations that are suggested by MGARCH models.

To substantiate our claim, we test for breaks in the otherwise constant correlation structure using a recent correlation change-point detection algorithm developed by Galeano and Wied (2014). This algorithm is a repeated application of the change-point test developed by Wied, Krämer, and Dehling (2012) and is able to identify level shifts that are associated with important financial or economic events. We illustrate this point in Figure 2, where we repeat the daily DCC correlations from the previous graph but superimpose the constant correlations including their level shifts. The algorithm of Galeano and Wied (2014) suggests that the underlying true correlation was initially constant during the five year period from 1990 to 1994. The change-point tests indicate a shift in the correlation structure in December 1994 which corresponds to the Mexican peso crisis. More correlation breaks followed: the Asian crisis in 1997, the burst of the Dot-com bubble which had its climax in March 2000, and the default of Lehman brothers in September 2008. The detection algorithm finds no evidence for additional correlation changes within each subsample. We therefore claim that much unlike conditional *volatility*, the true underlying *correlations* ρ are likely to be constant.[3]

<< Figure 2 about here >>

Our claim is in line with a number of empirical findings. Tse and Tsui (1999) investigate a number of tests aimed at detecting time-varying correlations through linear dependence in cross products of standardized residuals. They demonstrate that the tests correctly indicate model misspecification when a MGARCH model with constant conditional correlations (Bollerslev, 1990) is fitted to the data but the true DGP is a MGARCH model with dynamic conditional correlations. However, when applied to empirical data, most studies fail to detect linear dependence (Bollerslev, 1990; Tang, 1995; Tse, 2000). A number

[3] The assumption that daily correlations lie exactly on a straight line between breakpoints may be too strong. For instance, daily trading noise and price fluctuations in S&P500 and NASDAQ stocks is likely to generate small changes in the correlation structure even between breakpoints. However, the Wied, Krämer, and Dehling (2012) test indicates that those changes are not statistically significant and unlikely to reflect economically relevant changes. Our main arguments in this paper do not depend on the straight line assumption and have the same importance when we allow for correlation noise between breaks.

of studies have therefore relied on a constant correlation specification such as Bollerslev (1990) for European currencies quoted against the U.S. dollar, Longin and Solnik (1995) and Bera and Kim (2002) for national stock market returns, and Kroner and Ng (1998) for returns of small and large firm portfolios. Further evidence is provided by Tse (2000) who derives a Lagrange Multiplier test for constant conditional correlations. He finds this test to have high empirical power if the true DGP is a BEKK or a DCC-type model. Nevertheless, for several assets he fails to reject the null of constant conditional correlations.[4]

Given the substantial differences between the volatile DCC correlations in Figure 2 and the constant correlations that we claim describes the true underlying correlation structure, an important question is why the DCC parameters that govern the estimated correlation dynamics are often found to be statistically significant in empirical studies. Our empirical results show that statistical significance is much less important than expected. Although statistical significance decreases when we control for correlation breaks, the main difference in correlation dynamics is caused by a change in the size of parameter estimates. These size changes have important consequences for correlation dynamics because the interaction between correlation parameters is highly nonlinear. As a consequence, even small deviations from typical estimates can generate correlations that are either constant or fluctuate randomly at low volatility around a constant value.

The remainder of this paper is structured as follows. In the next section, we show for several asset classes that correlation breaks among daily returns are a common phenomenon. In section 3 we take a closer look at the impact of breaks on parameter estimates. When breaks are controlled for, parameter estimates often lie outside the narrow band that produces

[4] In contrast, comparable studies on the behavior of univariate GARCH models find that GARCH volatility adequately models the true data generating process (Bollerslev, Chou, and Kroner, 1992). Overall, the body of empirical literature over the last two decades lends support to the notion that extending the GARCH framework from volatilities to correlations is not as straightforward as previously thought.

meaningful correlation dynamics. A theoretical explanation for the results in our paper is explored in section 4. We derive an expression for the variance and autocovariance of DCC correlations when the true underlying correlations are constant. We show that this expression can be decomposed into a general term that is common to all parametric correlation estimators, and a model-specific term which adopts the unique characteristics of the underlying correlation specification. This allows us to demonstrate how DCC parameters cause artificial correlation dynamics. In section 5, we show under which circumstances the historical rolling window sample correlation is preferable to a DCC model. Section 6 summarizes our main results and gives our conclusions.

2 Correlation Breaks in Daily Asset Returns

In this paper, we argue that correlations are constant over time, but that financial shocks lead to breaks that shift the level of correlations. This section describes the empirical evidence concerning breaks in the correlation structure of financial assets. Over a 15-year period from 2000 to 2014, the majority of financial assets in our sample experience shocks that significantly shift the level of daily correlations. The presence of such correlation breaks has implications for the estimation of conditional correlation models. The existing literature on univariate volatility models shows that breaks in the volatility dynamics introduce a bias in the estimation which results in inaccurate volatility forecasts (Hamilton and Susmel, 1994; Hillebrand, 2005; Rapach and Strauss, 2008). However, the findings concerning volatility breaks cannot be simply extended to correlations. We show that correlation dynamics are exposed to model specific factors that are absent in univariate models of volatility.

2.1 The Dynamic Conditional Correlation (DCC) Model

Throughout this paper, our emphasis is on Engle’s (2002) popular mean-reverting Dynamic Conditional Correlation (DCC) model. The MGARCH family has grown considerably over the last years and a number of more complex models are better at dealing with structural breaks in correlations. For instance, Mittnik and Paolella (2000) propose a weighted maximum likelihood procedure that places less weight on observations in the more distant past. Pelletier (2006) introduces a regime-switching MGARCH model that allows for correlations that are constant within a regime but are different across regimes. However, the additional flexibility of these more advanced models comes at the cost of highly sensitive parameter estimates and extensive modeling and forecasting implementation. In contrast, DCC models are based on a parsimonious specification with correlation specific parameters that have an analogous interpretation to parameters of univariate GARCH models. In other words, we recognize the contribution of some of these more complex models but point out that so far they play only a minor role in most empirical settings. For the main arguments in our paper, which are about the dynamic correlations as they are used today, the simple canonical specifications are more relevant. Finally, DCC models generate conditional correlation dynamics which are similar to more complex MGARCH specifications such as BEKK (Engle, 2002; Engle and Colacito, 2006; Caporin and McAleer, 2012) or the corrected DCC of Aielli (2013). We therefore expect our results to hold also for other members of the MGARCH family.

For our analysis, we abstract from conditional mean effects, i.e. we assume that conditional means are constant. This assumption has no serious implications for daily data (Fleming, Kirby, and Ostdiek, 2001) and is common in the literature (West and Cho, 1995). Furthermore, and for the sake of simplicity, we only consider the bivariate case. This restriction has no implications for our results as DCC model parameters have the same impact on each component of the conditional correlation matrix. Hence, all our results apply to higher dimensions as well. The bivariate DCC model uses the specification

$$\rho_t = f(\mathbf{q_t}) = \frac{q_{12,t}}{\sqrt{q_{11,t} \cdot q_{22,t}}}, \tag{1}$$

where the elements of $\mathbf{q}_t = (q_{11,t}, q_{22,t}, q_{12,t})$ are functions of the standardized residuals $\{(e_{1,k}, e_{2,k})' : k < t\}$. The residuals $e_{i,t}$ are obtained as the GARCH residuals from the return equation $r_{i,t} = \sigma_{i,t} e_{i,t}$ and are typically associated with financial shocks or news (Engle and Ng, 1993). The q_t are estimated using the expression:

$$\hat{q}_{i,j,t} = \frac{1-a-b}{1-b}\vartheta_{i,j} + a\sum_{s=1}^{\infty} b^{s-1} e_{i,t-s} e_{j,t-s} = (1-a-b)\vartheta_{i,j} + a e_{i,t-1} e_{j,t-1} + b\hat{q}_{i,j,t-1} \tag{2}$$

with $a > 0$, $b > 0$, and $a + b < 1$. Intuitively, $q_{11,t}$ and $q_{22,t}$ can be regarded as auxiliary estimates of $E(e_{1,t}^2 | \mathcal{F}_{t-1})$ and $E(e_{2,t}^2 | \mathcal{F}_{t-1})$, respectively, where $\mathcal{F}_{t-1}$ denotes the information set available at time *t*-1. Similarly, $q_{12,t}$ is an auxiliary estimate of $E(e_{1,t} e_{2,t} | \mathcal{F}_{t-1})$. In line with this interpretation, Equation (1) simply states rescaling in such a way that $\hat{\rho}_t$ satisfies $-1 \leq \hat{\rho}_t \leq 1$. If the unconditional correlation between $e_{i,t}$ and $e_{j,t}$ is the same for all *t*, then a natural choice for the constant $\vartheta_{i,j}$ is $E(e_{i,t} e_{j,t})$ Although this definition of the constant does not assure that $E(\hat{\rho}_t) = E(e_{i,t} e_{j,t})$, most empirical applications are based on this specification. For this reason and because setting $\vartheta_{i,j} = E(e_{i,t} e_{j,t})$ considerably simplifies the analysis, we hence refrain from adjustments suggested in Aielli (2013) and refer to Caporin and McAleer (2008) for a detailed discussion. The parameter *a* models the sensitivity of q_t to the arrival of news $e_{i,t}$. If *a* is close to zero, correlations dynamics are insensitive to shocks and approximate a straight line. The parameter *a* therefore plays a special role in our paper. In contrast, the parameter *b* measures the persistence in correlations. A low *b* value generates correlations that fluctuate randomly at low volatility around a straight line.[5]

[5] An alternative measure of persistence that is sometimes used in the univariate GARCH literature is the sum of *a* and *b* (Hillebrand, 2005). Although the effectiveness of *b* depends on a reasonable value for *a*

2.2 A Correlation Breakpoint Test

To identify and locate change points in the correlation structure of financial assets we implement a simple and effective algorithm proposed by Galeano and Wied (2014) and Wied, Krämer, and Dehling (2012). In contrast to classical tests for breaks in time-series regression (e.g., Quandt, 1960; Davis, 1977) the methodology does not require possible break dates to be specified in advance but uses an algorithm for sequential breakpoint detection.[6]

This algorithm involves the following steps: Consider a sample of T observations of the returns vector $(r_{1,t}, r_{2,t})'$. Let ρ_t denote the true but unknown unconditional correlation between $r_{1,t}$ and $r_{2,t}$ at time t. The algorithm tests the null hypothesis of constant correlations against the alternative hypothesis of a change-point t^c, i.e.

$$H_0 : \rho_t = \rho \qquad \text{for all } t \in \{1,\ldots,T\} \tag{3}$$

versus

$$H_1 : \exists t^c \in \{1,\ldots,T-1\}. \text{ such that } \rho_{t^c} \neq \rho_{t^c+1}. \tag{4}$$

The procedure is based on the model-free fluctuation-type test (WKD test henceforth) originally proposed by Wied, Krämer, and Dehling (2012). The test statistic is defined as

$$Q_T := \hat{D} \max_{2 \le t \le T} \frac{t}{\sqrt{T}} \,|\, \hat{\rho}_t - \hat{\rho}_T \,|, \tag{5}$$

where $\hat{\rho}_t$ is the sample correlation over the period 1 to t. The purpose of the scalar coefficient $\hat{D}$ is to rescale the volatility of $\hat{\rho}_t$ which tends to be higher at the beginning of the sample when only a few observations are available. The coefficient $\hat{D}$ is described in

(somewhere between 0.02 and 0.06) the actual persistence is governed by the size of *b*. We therefore rely on *b* as a measure of persistence throughout the paper.

[6] An alternative correlation break point methodology is the test proposed by Andreou and Ghysels (2002, 2003). The results in our paper do not change significantly under this alternative test. To conserve space, we do not report the results here but instead focus on the test of Wied, Krämer, and Dehling (2012).

more detail in Appendix B. Under the null hypothesis and several reasonable moment and dependency restrictions, the test statistic Q_T is asymptotically Kolmogorov distributed (Wied, Krämer, and Dehling, 2012, Theorem 1).[7] If Q_T stays below the upper critical value the null hypothesis of constant correlation cannot be rejected and the algorithm stops. Otherwise, H_0 is rejected and the correlation sample contains at least one change-point t^c. The estimator for the single change-point is defined as

$$t^c = \arg\max_t \hat{D} \frac{t}{\sqrt{T}} \, | \hat{\rho}_t - \hat{\rho}_T \, |. \tag{6}$$

To identify further change-points, the sample is split into the two subsamples $[1,...,\hat{t}^c]$ and $[\hat{t}^c + 1,...,T]$. These subsamples are then both tested individually. This procedure is repeated until no further change-points are detected. Galeano and Wied (2014) demonstrate that the presence of multiple change-points can affect the test's efficiency in identifying the true number of change points. The last step of the algorithm therefore consists of a refining process in which the vector of the *n* detected change-points $\tau = [\hat{t}_1^c,...,\hat{t}_n^c]$, sorted in ascending date order $\hat{t}_1^c \leq ... \leq \hat{t}_n^c$, is verified in subsamples containing only a single change point. For the implementation of the refining process we define the first observation of the sample as $\hat{t}_0^c = 0$, the last observation as $\hat{t}_{n+1}^c = T$, and form the subsamples $[\hat{t}_{i-1}^c + 1,...,\hat{t}_{i+1}^c]$ for $i = 1,...,n$. Each subsample starts at the first observation following the previous change-point $\hat{t}_{i-1}^c$, includes change point $\hat{t}_i^c$, but ends just before the next change-point $\hat{t}_{i+1}^c$. These subsamples are tested individually. If the null hypothesis is not rejected the change-point contained in the subsample is removed from τ.

[7] See assumptions A.1 to A.5 in Wied, Krämer, and Dehling (2012). In particular, it is assumed that $\{(r_{1,t}, r_{2,t})'\}$ is near-epoch dependent. For an extensive discussion see Davidson (1994, Ch. 17).

We give a brief example to illustrate the test procedure. We test for a break in the daily correlation between the returns of the FTSE100 index and the returns of the Dutch AEX index. If we test the full sample from 01/03/2000 to 11/28/2014 we detect one significant change-point at 01/17/2008. In the next step, we split the data in the two subsamples [01/03/2000–1/17/2008] and [01/18/2008–11/28/2014]. We test the two subsamples individually and find another change-point in the first subsample at 08/31/2001. The test statistic in the second subsample is insignificant. The presence of the second change-point interferes with the test statistic for the first change-point that was detected using the entire sample. The last step therefore involves a refining process in which we test the subsamples [01/03/2000–01/17/2008] and [09/01/2001–11/28/2014]. The test statistics for both subsamples remains significant and confirms the presence of both change-points: $\tau =$ [08/31/2001, 01/17/2008]. Galeano and Wied (2014) demonstrate that this procedure detects the correct number of correlation change-points.

We apply the WKD test to the daily returns of 40 assets over the period 01/03/2000 to 12/31/2014 (3914 obs.). Our data covers the asset classes stocks, bonds, commodities, and currencies. Each asset class is represented by 10 major indices or currency pairs. Appendix C lists the constituents in detail. We obtain $1/2 \cdot n(n-1) = 780$ correlation time series to be tested for breaks. Panel A in Figure 3 shows the distribution of breaks over time. Intuitively, correlation breaks should cluster around dates that are associated with important financial shocks. Panel A indicates that this is in fact the case. The two events that appear to have influenced correlations most are the failure of two Bear Stearns funds in July 2007 and the bankruptcy of Lehman Brothers in September 2008. If we look at the table of correlation breaks in Panel B we see that 420 return pairs, or more than half of the assets in our data experienced exactly one correlation break. More than two correlation breaks is much less common. In 26% of cases, the WKD test did not identify a significant change in correlations.[8] Finally, Panel C shows how correlations change after a break. Since small changes are likely to be statistically insignificant the distribution shows a distinct bimodal shape. Financial crises tend to increase the comovement among assets which can explain the higher positive mode. In fact, the majority, or 61% of correlation changes are positive. The largest negative drop in average correlations is -0.68. The largest positive jump is as high as 0.58. The average positive or negative correlation change is around 0.18. From our findings in Figure 3 we conclude that correlation breaks in financial assets is a common phenomenon and that the change in correlations following a break is often large. In the following section, we investigate the consequences of breaks on DCC parameter estimates which govern the dynamics of conditional correlations.

<< Figure 3 about here >>

3 The Impact of Correlation Breaks on DCC Parameter Estimates

Over the 15 year period from 2000 to 2014, the majority of financial assets experienced at least one correlation break. If correlation breaks are a prevalent characteristic of financial assets, the question is how this affects the parameters that govern the correlation dynamics. To answer this question, we use the $n = 40$ assets from the previous section and obtain $1/2 \cdot n(n-1) = 780$ correlation time series. First, we collect the DCC parameter estimates over the full sample from 03/01/2000 to 12/31/2014 (3,914 obs.). In a second step, we re-estimate the parameters running the model over the subsamples between correlations breaks.[9] We obtain 780 DCC parameter pairs for the full samples and 1,596 parameter pairs for the subsamples. In the following, the full sample estimates serve as our control group while the

[8] This appears to be particularly the case for assets that had very low correlations to begin with.

[9] We exclude five observations before and after the break to remove possible transition effects that occur around the break date.

subsample estimates are our treatment group. To allow for a direct comparison between the two groups we need to ensure that the full sample correlations contain at least one correlation break. In addition, we exclude correlations that are already constant in full samples. This occurred in a number of cases in which the *DCC a* parameter was close to zero.[10] We discuss this important situation in more detail in Section 4. Finally, we remove subsamples that contain less than 500 observations to ensure that our results are not driven by small sample windows. Our final sample consists of 355 full sample correlations and 802 subsample correlations.

Panel A of Figure 4 shows the descriptive statistics of DCC parameters and compares full samples to subsamples. We find an average value for *DCC a* of 0.021 and for *DCC b* of 0.97 which are in line with findings from other studies. For instance, Engle and Sheppard (2001) investigate the daily returns of the DJIA index and report 0.01 and 0.96 for *DCC a* and *b*, respectively. Engle and Colacito (2006) investigate the daily returns of the S&P 500 and the 10-year U.S. bond futures contract and report 0.022 and 0.973 for *DCC a* and *b*. Measured at the 95% confidence level, our parameter estimates are statistically significant in 91% of all cases.

<< Figure 4 about here >>

When we compare these numbers to the estimates found in subsamples the average coefficients appear to be quite similar. The average *DCC a* parameter is close to the full sample estimate while the *DCC b* estimate is somewhat lower. This observation is in line with Rapach and Strauss (2008) and Hillebrand (2005) who find that the persistence parameter β for univariate GARCH models decreases after accounting for structural breaks in volatility. The main change in subsamples parameters, however, does not take place in the

[10] We impose the parameter restrictions $0.01 < a < 0.06$ and $0.8 < b < 0.99$ which will generate a typical dynamic correlation behavior.

average estimate but in its distribution. For instance, subsample *DCC a* estimates now range between 0 and 0.244 and *DCC b* values range between 0 and 0.997. Panel B of Figure 4 illustrates the impact of correlation breaks on the parameter distribution for different asset classes in our sample. The distribution of *DCC a* parameters shows a number of positive outliers, in particular in cases when the correlations are measured among stocks, bonds, or between mixed assets types. This finding is even stronger when we look at the change in distribution of the *DCC b* parameter. A significant part of the distribution now covers parameters below 0.5 which leads to a low persistence in the correlation dynamics. To conclude, estimating DCC models in subsamples that contain no breaks has subtle but important consequences for DCC parameter estimates. However, it is unclear how the changes in DCC parameters affect correlation dynamics. We will explore this issue in the following section.

4 The Impact of Correlation Breaks on Correlation Dynamics

In this section, we show how breaks in the correlation structure of financial assets affect the dynamics of correlation estimators. We derive an expression for the autocovariance function of conditional correlations. This expression shows how the autocovariances can be separated into a general variance part and a model part which explicitly depends on the parameterization of the correlation process. In this context, we compare the results from the DCC model to two simple correlation estimators that are popular in practice: the fixed parameter exponentially weighted moving average (EWMA) estimator and the historical sample correlation estimated in a rolling window.[11] In a number of cases, these simple alternatives will perform better than a MGARCH-type correlation estimator.

[11] The EWMA estimator uses fixed parameters proposed by the RiskMetrics group and is therefore sometimes called the “RiskMetrics model” (Rapach and Strauss, 2008).

4.1 Dynamic Correlation Estimators

Our first estimator is the *rolling window (RW) sample correlation*. The (historical) sample correlation of asset returns is a simple and popular estimator in applied finance. However, it is not just an ad hoc way to measure dynamic correlations. As shown in Foster and Nelson (1996) there are several DGPs for which an appropriately specified rolling window estimator is optimal. We follow the literature and use this estimator as a benchmark to be tested against the performance of more sophisticated MGARCH models (Engle, 2002). Again, we can facilitate comparison among estimators by expressing the RW correlation in terms of $\hat{q}_{i,j,t}$, which in the case of the rolling window estimator is a function of *n* equally weighted observations ranging from $t-n$ to $t-1$:

$$\hat{q}_{i,j,t} = n^{-1}\sum_{s=1}^{n} e_{i,t-s}e_{j,t-s} \ . \tag{7}$$

Our second correlation estimator is the fixed parameter *Exponentially Weighted Moving Average (EWMA)* estimator. The implementation of this estimator is just slightly more elaborate than a rolling window correlation. The dynamics generated by the EWMA model are very similar to MGARCH models but the parameters are given rather than being estimated.[12] RiskMetrics suggests modeling the dynamics in the daily asset return covariance using a persistence parameter $\lambda = 0.94$ (Longerstaey and More, 1995). The response to shocks is measured by the remaining $\left(1-\lambda\right) = 0.06$

$$\hat{q}_{i,j,t} = \left(1-\lambda\right)\sum_{s=1}^{\infty}\lambda^{s-1}e_{i,t-s}e_{j,t-s} = (1-\lambda)e_{i,t-1}e_{j,t-1} + \lambda\hat{q}_{i,j,t-1} \tag{8}$$

The importance of the standardized shocks from both assets $e_{i,t-s}e_{j,t-s}$ decreases exponentially, thereby emphasizing the information provided by current observations relative to past observations. For the analysis in our paper, the EWMA model is useful in two ways.

[12] When the parameters are estimated the EWMA becomes the Integrated Dynamic Conditional Correlations (IDCC) estimator (Engle 2002).

First, the effort of implementing the EWMA estimator is somewhere between a rolling window estimator and the more sophisticated MGARCH models. Second, since the persistence parameter λ and the shock sensitivity $1-\lambda$ sum up to one, the resulting correlations are non-stationary, so that shocks can generate permanent level shifts in dynamic correlations (Engle, 2002). This feature is important since economic disruptions are reflected in many financial time series. Although the EWMA model suffers from similar shortcomings as the DCC model, it should in principle be particularly suited for this purpose.

Our last estimator is the *Dynamic Conditional Correlations (DCC)* estimator that was already presented in section 2.1. Because of the constant in the function of $q_{ij,t}$, Engle's (2002) mean-reverting DCC specification can be considered as an extension of the EWMA model. For the sake of completeness, we repeat the expression for $\hat{q}_{i,j,t}$ here:

$$\hat{q}_{i,j,t} = \frac{1-a-b}{1-b}\vartheta_{i,j} + a\sum_{s=1}^{\infty} b^{s-1} e_{i,t-s} e_{j,t-s} = (1-a-b)\vartheta_{i,j} + ae_{i,t-1}e_{j,t-1} + b\hat{q}_{i,j,t-1} \tag{9}$$

We will now investigate how changes in the correlation parameters govern the dynamics of correlation estimators.

4.2 Anatomy of Conditional Correlation Dynamics

In this section, we show that the volatile pattern that is typically observed when applying conditional correlation measures is to a large extent artificial. We demonstrate that correlation dynamics depend on the specification of the correlation model. The impact of the model in turn is amplified by the level of the underlying correlation structure. The volatility of the estimated dynamic correlation $\hat{\rho}_t$ is highest when the true underlying correlation ρ is zero and diminishes as ρ approaches ± 1. The key finding is that estimated correlations contain a fluctuation component that is unrelated to the correlation parameters. In the following we will formally demonstrate this effect. We start by considering a DGP that produces constant correlations. In terms of $\mathbf{q_t}$ as in Equation (8) above we define:

$\rho_t = f(\mathbf{q_t}) = q_{12,t} \big/ \sqrt{q_{11,t} q_{22,t}}$, where $\mathbf{q_t} = (1,1,\rho)$. Since the true correlation is constant, it follows that $\rho = E\left(e_{1,t}e_{2,t} \,|\mathcal{F}_{t-1}\right) = E\left(e_{1,t}e_{2,t}\right)$ and the variance and all autocovariances of conditional correlations are zero.

To focus on the correlation effect, we assume that we have a correctly specified model for the conditional return volatility, so that the standardized residuals e_t are homoscedastic and normally distributed:

$$\left(e_{1,t}e_{2,t}\right)' \sim i.i.d.N\left(\begin{pmatrix}0\\0\end{pmatrix},\begin{pmatrix}1 & \rho\\ \rho & 1\end{pmatrix}\right). \tag{10}$$

In the following, we will simplify the analysis and use the first-order Taylor expansion of $f(\widehat{\mathbf{q}}_t)$ around $E(\mathbf{q}_t) = \varphi = (1,1,\rho)$ to approximate $Cov(\hat{\rho}_t, \hat{\rho}_{t-s})$. A Monte Carlo simulation in Appendix D shows that a reasonable choice of model parameters approximates the exact analytical expression for $Cov(\hat{\rho}_t, \hat{\rho}_{t-s})$ quite well.[13] The Taylor series expansion of $\hat{\rho}_t^*$ can be expressed as

$$\hat{\rho}_t^* = f(\varphi) + \frac{\partial f(\varphi)}{\partial f \varphi'}(\widehat{\mathbf{q}}_t - \varphi). \tag{11}$$

We will therefore approximate $Cov(\hat{\rho}_t, \hat{\rho}_{t-s})$ by

$$Cov(\hat{\rho}_t^*, \hat{\rho}_{t-s}^*) = \frac{\partial f(\varphi)}{\partial f \varphi'} Cov(\widehat{\mathbf{q}}_t, \widehat{\mathbf{q}}_{t-s}) \frac{\partial f(\varphi)}{\partial f \varphi}. \tag{12}$$

Proposition 1: *Let* $\{(e_{1,t,}e_{2,t})'\}$ *be a bivariate i.i.d. process as defined in (10) with* $|\rho| < 1$ *and* $s \geq 0$, *and define* $\mathbf{\Omega} = 2\begin{pmatrix}1 & \rho^2 & \rho\\ \rho^2 & 1 & \rho\\ \rho & \rho & \frac{1}{2}(1+\rho^2)\end{pmatrix}$.

If $\widehat{\mathbf{q}}_t$ *follows the definition in (9) then*

(i) $Cov(\widehat{\mathbf{q}}_t, \widehat{\mathbf{q}}_{t-s}) = \gamma^{DCC}(a,b,s)\mathbf{\Omega}$, *where* $\gamma^{DCC}(a,b,s) = \frac{b^s a^2}{1-b^2}$.

If $\widehat{\mathbf{q}}_t$ *follows the definition in (8) then*

[13] For further examples, see Kwan (2008) and the references therein.

(ii) $Cov(\widehat{\mathbf{q}}_t, \widehat{\mathbf{q}}_{t-s}) = \gamma^{EWMA}(\lambda, s)\mathbf{\Omega}$, *where* $\gamma^{EWMA}(\lambda, s) = \frac{\lambda^s(1-\lambda)^2}{1-\lambda^2}$.

If $\widehat{\mathbf{q}}_t$ *follows the definition in (7) then*

(iii) $Cov(\widehat{\mathbf{q}}_t, \widehat{\mathbf{q}}_{t-s}) = \gamma^{RW}(n, s)\mathbf{\Omega}$, *where* $\gamma^{RW}(n, s) = \frac{n-s}{n^2}$ *for* $s < n$ *and* $\gamma^{RW}(n, s) = 0$ *for* $s \geq n$.

Proposition 1 implies that $Cov(\hat{\rho}_t^*, \hat{\rho}_{t-s}^*)$ contains a true unconditional correlation component $\frac{\partial f(\varphi)}{\partial f \varphi'} \mathbf{\Omega} \frac{\partial f(\varphi)}{\partial f \varphi}$, and a model-specific multiplier γ^{DCC}, γ^{EWMA}, and γ^{RW}. It is important to note that $\mathbf{\Omega}$ is unrelated to any model parameters. Fluctuations over time are therefore an inherent part of correlation dynamics.

Proposition 1 allows us to express $Cov\left(\hat{\rho}_t^*, \hat{\rho}_{t-s}^*\right)$ in a single number. Let $\kappa(\rho) = (1-\rho^2)^2$. For the case that $\hat{q}_t$ follows the DCC model we obtain

$$Cov(\hat{\rho}_t^*, \hat{\rho}_{t-s}^*) = \gamma^{DCC}(a, b, s)\kappa(\rho).$$

For the case that $\hat{q}_t$ follows the EWMA model we obtain

$$Cov(\hat{\rho}_t^*, \hat{\rho}_{t-s}^*) = \gamma^{EWMA}(\lambda, s)\kappa(\rho).$$

Finally, for the case that $\hat{q}_t$ follows the RW model we obtain

$$Cov(\hat{\rho}_t^*, \hat{\rho}_{t-s}^*) = \gamma^{RW}(n, s)\kappa(\rho).$$

For the discussion of correlation dynamics we focus on these expressions of $Cov\left(\hat{\rho}_t^*, \hat{\rho}_{t-s}^*\right)$.

4.3 The Impact on Correlation Dynamics

We have demonstrated that $Cov(\hat{\rho}_t^*, \hat{\rho}_{t-s}^*)$ has a model-independent component $\kappa(\rho)$ that is fully determined by the size of the true underlying correlation ρ, and a model multiplier γ. In other words, a dynamic correlation estimator $\hat{\rho}_t$ generates spurious dynamics even when the true underlying correlation ρ is constant.[14] With $|\rho| < 1$ and $\gamma > 0$, setting the lag s to zero results in the variance of $\hat{\rho}_t^*$: $Cov\left(\hat{\rho}_t^*, \hat{\rho}_t^*\right) = Var\left(\hat{\rho}_t^*\right) > 0$. The definition of $\kappa(\rho) = (1-\rho^2)^2$ shows that, as long as returns are not perfectly correlated, $\kappa(\rho)$ is always positive and has a global maximum at $\rho = 0$. As a consequence, the estimated correlation $\hat{\rho}_t$ contains daily fluctuations even when the true correlation does not. In addition, $\hat{\rho}_t$ depends on lagged values when $Cov\left(\hat{\rho}_t^*, \hat{\rho}_{t-s}^*\right)$ is significantly positive for lags $s > 0$. A high persistence can give the pattern in $\hat{\rho}_t$ a spurious dynamic behavior that some researchers have interpreted as cycles (e.g., Cai, Chou, and Li., 2009; Pukthuanthong and Roll, 2011).[15]

Given the correlation parameters (a and b in the DCC model, λ in the EWMA model, and n in the rolling window model) the relationship between the volatility of the correlation estimate $\sigma_{\hat{\rho}} \approx \sqrt{Var\left(\hat{\rho}_t^*\right)} = \sqrt{\gamma\kappa(\rho)}$ and the level of the true underlying correlation ρ is described by an inverse parabolic relationship. A high correlation level such as ±0.95 generates stable correlation dynamics irrespective of the underlying model specification. If the level of correlation decreases from 0.95 to 0.50 the volatility of $\hat{\rho}_t$ increases by a factor of 6. If the underlying correlation decreases further to 0, the volatility of $\hat{\rho}_t$ increases by another 33%. Again, this increase in volatility occurs for all model specifications and parameter choices. In empirical applications, the pronounced fluctuations

---

[14] Technically, $\hat{\rho}_t$ will be zero if $\gamma = 0$. We can ignore this situation since this describes the trivial case when all parameters driving the correlation dynamics are zero. Note that a positive rolling window multiplier requires $s < n$.

[15] We note several similarities between our findings and those on rolling windows and ARMA-type processes provided elsewhere (e.g., Lütkepohl, 2006). However, except for some simulation results reported in Aielli (2013), we are not aware of any paper considering the autocovariance structure of conditional correlations.

in correlation dynamics are often interpreted as the result of incoming financial news (Christiansen, 2000; Cappiello, Engle, and Sheppard, 2006). A simple and more likely explanation is that assets share a low level of correlation. We can test whether this relationship can also be found in empirical data. To obtain an estimate of the volatility in the correlation measure, $\hat{\sigma}_{\hat{\rho}}$, we estimate dynamic correlations $\hat{\rho}_t$ for our 40 assets and take the sample standard deviation. We can obtain a measure of ρ by taking the average over the time series of $\hat{\rho}$.[16] Panel A of Figure 5 plots $\hat{\sigma}_{\hat{\rho}}$ on the *y*-axis against the level of correlation on the *x*-axis. The solid line shows the theoretical relationship of $\hat{\sigma}_{\hat{\rho}}$ as derived in the previous section emphasizing that $\hat{\sigma}_{\hat{\rho}}$ is an inverse parabolic function of ρ. For instance, $\hat{\sigma}_{\hat{\rho}}$ in the DCC model is generated by $\hat{\sigma}_{\hat{\rho}} = \sqrt{\gamma^{DCC} \cdot \kappa(\rho)} = \sqrt{0.03^2 / (1-0.96^2) \cdot (1-\rho^2)^2}$, where we have used typical DCC parameters $DCC\, a = 0.03$ and $DCC\, b = 0.96$. The humped shaped relationship is shown in the left graph of Panel A. For comparison, the dashed line with 95% confidence bands shows an estimated nonparametric relationship based on the actual data. The empirical relationship matches the theoretical one, lending support to the notion that dynamic correlations are likely to be more imprecise when the underlying correlation is close to zero. The EWMA model in the right graph of Panel A verifies this observation. Although we lack data for extreme negative correlations, we find strong evidence that the relationship holds for large positive correlations. An increasing variation in the observations around $\rho = 0$ suggests that the link between $\hat{\sigma}_{\hat{\rho}}$ and ρ is less clear when assets are uncorrelated.

<< Figure 5 about here >>

[16] The presence of correlation breaks is likely to change the model multiplier γ. To separate this effect from the hump shaped function of the model-independent component $\kappa(\rho)$, we base our dynamic correlation estimates on subsamples.

The theoretical relationship is derived under our assumption that true correlations within subsamples are constant. To illustrate how the observed relationship would behave in a perfectly constant environment, we simulate daily DCC correlations under the restriction that the true underlying errors $\left(e_{1,t}, e_{2,t}\right)'$ remain unchanged over time. This situation is shown in the left graph of Panel B. By construction, the theoretical curve now perfectly fits the point cloud. We note some interesting similarities between the humped shaped relationship derived under the controlled simulation with the one observed in the actual data. First, the general form, with high fluctuations in ρ when assets are uncorrelated and decreasing volatility as ρ approaches ± 1, are clearly visible in the actual financial data. Second, the uncertainty concerning $\hat{\sigma}_{\hat{\rho}}$ is highest for uncorrelated assets. We interpret these similarities as an additional indicator that correlations in financial data are likely to be constant when structural breaks in correlations are accounted for.[17]

Our findings concerning the volatility in $\hat{\rho}_t$ do not extend to univariate GARCH models. We can repeat our analysis based on univariate GARCH volatility $\hat{\sigma}_t$ instead of $\hat{\rho}_t$. To collect observations on the level and volatility of $\hat{\sigma}$, we apply a volatility breakpoint test and measure the average sample volatility $\bar{\hat{\sigma}}$ and the volatility of the GARCH volatility $\hat{\sigma}_{\hat{\sigma}}$ within subsamples. For detecting volatility breaks, we apply the test developed in Inclán and Tiao (1994).[18] The right graph in Panel B shows that the relationship for $\hat{\sigma}$ appears linear and is strictly positive: higher levels of σ are associated with higher fluctuations in $\hat{\sigma}$.

---

[17] Of course, some differences are to be expected given that in practice, underlying correlations are not perfectly constant and are subject to differences DCC parameters and sample size.

[18] Rapach and Strauss (2008) propose an adjusted Inclán-Tiao test that is more effective in the presence of GARCH effects. For our purpose, the adjustment is of minor importance since our primary goal is to collect data on the level and volatility of $\hat{\sigma}$, and not to detect the correct break point date.

Hence, our findings concerning the behavior of correlations differ from previous results for univariate volatility models (e.g., Rapach and Strauss, 2008).

The humped shape function described by $\kappa(\rho)$ is a general result. However, it cannot show how breaks in the correlation structure transmit to DCC parameter values and ultimately affect the volatility of $\hat{\rho}$. The link between correlation breaks and $\hat{\sigma}_{\hat{\rho}}$ is established through the model multiplier γ: correlation breaks distort correlation parameter estimates which in turn directly determine γ. In Section 3 we found only small average changes in estimates of $DCC\ a$ and b. Comparing full samples and subsamples, the average $DCC\ b$ decreased from 0.970 to 0.836, and the average $DCC\ a$ actually increased slightly from 0.021 to 0.027. At first glance, none of these changes appear to be particularly large. However, we will show in the following that even small parameter changes can have a substantial impact on $\hat{\sigma}_{\hat{\rho}}$ if they move outside a narrow range. In the extreme case when $DCC\ a$ or b estimates are close to zero, the generated correlations $\hat{\rho}_t$ are constant. We find this to be the case in a number of subsamples. To compare DCC parameter estimates in full samples from those obtained in subsamples we proceed in two steps. We first concentrate on the full sample and select asset correlations from which typical estimates of $DCC\ a$ and b values can be obtained. As before, the full samples contain daily data from 01/03/2000 to 12/31/2014 (3914 obs.). We then take the same assets but re-estimate the DCC parameters over the subsamples where we follow our previous approach and define subsamples to lie on both sides of a correlation break point. Panel A in Figure 6 shows pairs of $DCC\ a$ and b estimates. The full sample estimates in the left graph were selected to be within a range of $0.01 < DCC\ a < 0.06$ and $0.8 < DCC\ b < 0.99$. Only parameter combinations that lie within this range generate typical dynamic correlation. The range is indicated by a green background to highlight that the area of allowed parameters is small relative to the theoretically possible parameter space. The right graph shows the distribution of DCC estimates when re-estimated over subsamples. The estimates are based on the same asset pairs that were used in the full sample analysis and are therefore directly comparable. We exclude subsamples with less than 500 observations to remove small sample effects on the parameters. A large fraction of the parameter estimates now lie outside the range of typical parameter values. A number of *DCC b* values are smaller than 0.5 and some are even zero.

<< Figure 6 about here >>

In Panel B we illustrate how parameter estimates outside the normal range impact the correlation dynamics. The left graph shows a generated correlation when *DCC a* is close to zero. As expected, the generated correlations are constant. The right graph shows the situation when *DCC a* takes on a typical value but *DCC b* is 0.5. The generated correlation is quasi constant with small fluctuations around a straight line. We can summarize our findings concerning parameter changes as follows: The typical dynamic pattern of $\hat{\rho}_t$ that has become a stylized fact for many financial assets requires that both, $DCC\ a$ and b lie within a narrow range.[19] Parameter values outside this range lead to correlations that lack typical dynamics. When estimated over subsamples that do not contain a break, many of the correlations turned out to be constant. Our findings suggest that many correlation dynamics are spurious and disappear once correlation breaks are controlled for.

It is instructive to investigate how the dynamics in $\hat{\rho}_t$ respond to the interaction of $DCC\ a$ and b. We show that this interaction is strongly nonlinear so that seemingly small changes in model parameters can have significant effects. In particular, the observed decrease in $DCC\ b$ from 0.970 in full samples to 0.836 in subsamples has important implications for the dynamics of $\hat{\rho}_t$. Panel A of Figure 7 shows the location of full sample and subsample

[19] The results also hold in the case of the EWMA model for various λ.

DCC parameters on the $Var\left(\hat{\rho}_t^*\right)$ surface. The surface shows a distinct upward slope in for cases of high $DCC\ a$ and b values. The full samples estimates with $DCC\ a = 0.021$, $DCC\ b = 0.970$, and $DCC\ a + DCC\ b = 0.991$ constitute one such combination that generate large fluctuations in $Var\left(\hat{\rho}_t^*\right)$. For the full sample, we find $Var\left(\hat{\rho}_t^*\right)$ to be 0.004. The upward slope illustrates the "narrow band" that we mentioned before. On the other hand, $Var\left(\hat{\rho}_t^*\right)$ quickly converges towards zero if one DCC parameter decreases just slightly. The location of the subsample DCC parameters shows a marginally higher $DCC\ a$ value of 0.027 that is more than compensated by a significantly lower $DCC\ b$ value of 0.836. The sum of both DCC parameters is 0.863 and therefore significantly below one. The location on the surface indicates that these values produce much less volatile estimate of $\hat{\rho}_t$. In fact, our estimate for $Var\left(\hat{\rho}_t^*\right)$ in subsamples is just 0.001, a quarter of its full sample size. This supports the notion that DCC correlations are constant in subsamples. From the findings in Panel A, we conclude that due to the nonlinear interaction of DCC parameters, even small deviation can have important implications for the variation in $\hat{\rho}_t$.

Panel B shows how the findings concerning the variance of $\hat{\rho}_t$ also extend to the autocovariance and therefore the dynamics of $\hat{\rho}_t$. To highlight the impact of $DCC\ b$ on various autocovariance lags *s*, the value for $DCC\ a$ is fixed at 0.02. The shape of the autocovariance surface shows that $\hat{\rho}_t$ has very short or no memory for most parameter combinations. Significant dynamics only emerge for $DCC\ b$ values that are large, so that the sum of $DCC\ a$ and b are close to one. Again, the average parameter location in full samples is sufficiently close to one to produce the distinct dynamics that are typical for correlation estimates of many financial time series. In contrast, average subsample DCC parameters produce correlations with little serial correlation. The findings in Panels A and B indicate that when controlling for breaks, dynamic conditional correlation estimates show little variations and no significant dynamics. The implication is that the nature of correlations is constant.

5 Volatility Ratios

Like variances, correlations are unobserved and need to be estimated. The absence of a true observed correlation complicates model comparison in empirical applications. Engle and Colacito (2006) propose a method that allows for an effective comparison of correlation models within the portfolio setting. The idea is to use portfolio variance as a measure of the effectiveness of a dynamic correlation model where lower variance indicates a better correlation model. Consider the standard portfolio optimization problem

$$\min_{w_{i,t}} \mathbf{w}'_{i,t}\mathbf{H}_{i,t}\mathbf{w}_{i,t} \quad s.t.\, \mathbf{w}'_{i,t}\mu = \mu_0\,, \tag{13}$$

where $\mathbf{H}_{i,t}$ is the conditional covariance matrix of model i at time t, μ is the vector of portfolio weights and $\mu_0 > 0$ is the required target return. Campbell, Lo, and MacKinley (1997) show that the solution and therefore the optimal portfolio weights can be estimated by $\mathbf{w}_{i,t} = \left(\mathbf{H}_{i,t}^{-1}\mu\right)\big/\left(\mu'\mathbf{H}_{i,t}^{-1}\mu\right)\mu_0$. The volatility of the portfolio return $\mathbf{w}'_{i,t}\mathbf{r}_t$ can then be obtained as $\hat{\sigma}_{i,t} = \sqrt{\mathbf{w}'_{i,t}\mathbf{H}_{i,t}\mathbf{w}_{i,t}}$. An efficiently estimated dynamic covariance matrix $\mathbf{H}_{i,t}$ will be reflected in a low portfloio volatility $\hat{\sigma}_{i,t}$. A comparison of covariance matrix estimators based on this approach has been applied for instance in DeMiguel, Garlappi, and Uppal (2009) but was entirely based on constant moments.

To compare portfolio volatilites Engle and Colacito (2006) form volatility ratios $VR_{i,t}$. In the ideal case where the true covariance matrix $\mathbf{\Omega}_t$ is known the volatility ratio would be

$$VR_{i,t} = \frac{\sqrt{\mathbf{w}'_{i,t}\mathbf{H}_{i,t}\mathbf{w}_{i,t}}}{\sqrt{\mathbf{w}_t^{*}\mathbf{\Omega}_{i,t}\mathbf{w}_t^{*}}}\,, \tag{14}$$

By construction, the volatility ratio in Equation (14) is larger than one and indicates the excess portfolio volatility that is based on the estimate $\mathbf{H}_{i,t}$ rather than the true correlation matrix $\mathbf{\Omega}_t$. The extent to which $VR_{i,t}$ exceeds one indicates the inefficiency of the dynamic covariance estimator. Since true correlations are unobservable in practice, Engle and Colacito (2006) consider a version of $VR_{i,t}$ that is based on the different model specifications for $\mathbf{H}_{i,t}$:

$$\widehat{VR}_{i,t} = \frac{\hat{\sigma}_{i,t}}{\min\left(\hat{\sigma}_{1,t},\cdots,\hat{\sigma}_{n,t}\right)} \ , \tag{15}$$

We follow this approach and consider the $n = 3$ correlation models DCC, RW and EWMA. To evaluate the performance of our three models in terms of portfolio variance we use the same 40 asset data set that was employed in previous sections. Our focus is on the model performance in samples that contain breaks and more stable situations that do not contain any breaks. One potential issue is the different sample size that can influence estimation results. For instance, a larger non-break sample could appear to produce smaller portfolio volatilities because the large number of observations leads to more precise model parameters. To circumvent this problem we select break and non-break samples of equal size. To illustrate this a bit further, Panel A of Figure 8 shows the sample selection process for the correlation between the stock indices of Italy (MIB) and the Netherlands (AEX). For this sample, we detect a correlation break point at observation 198, another at observation 430, and a third at observation 2,814. The third observation is a suitable break partition and we select a 1,000 observation window from observation 2,314 to 3,314 with the breakpoint in the center of that window. The data prior to the break window contain sufficient observation to select another 1,000 non-break observation window for comparison. We analyze all other asset pairs in this way and collect 429 break and non-break partitions of size 1,000.

<< Figure 8 about here >>

The portfolio variance is not only a function of the estimated covariance matrix but also depends on the expected return vector μ that enters the optimization as an input. Although the variance does not appear to respond very strongly to this assumption, we follow Engle and Colacito (2006) and compute volatility ratios over a range of expected returns. Panel B of Figure 8 shows the percentage of cases in which the smallest portfolio variance is generated by the DCC model and hence has a volatility ratio of one. Among the three correlation models, the DCC model performs well in situations that do not contain a structural break producing the lowest portfolio variance in 60% to 80% of all cases. In samples that contain a correlation break, the DCC parameters are biased and the portfolio performance decreases. Still, the overall performance of the DCC is quite remarkable compared to its competitors. However, the break samples that form the basis for the results in Panel B only test for the presence of a statistically significant break whereas the DCC parameters are likely to respond also to the size of the break. In Panel C we look at model performance conditioning on the size of the break indicated on the *x*-axis of the graph. For economically small correlation breaks up 0.4 the DCC model produces lower portfolio variances than the rolling window or the EWMA model. However, the performance of the DCC model deteriorates quickly as the break size increases. For instance, for small breaks of less than 0.1, DCC is the best model in 65% of all cases. For larger breaks between 0.4 and 0.5, the DCC is the best choice in 33% of all cases. For large correlation breaks of more than 0.5, the distorting effect on the DCC correlation is so strong that the simple rolling window estimator leads to better portfolio performance. Multivariate GARCH models like DCC are often praised for their dynamic flexibility to accommodate changes in the return pattern. Our results indicate that in the presence of correlation breaks a rolling window estimator may perform better despite its simplicity.

6 Conclusion

In this paper, we provide empirical evidence that daily correlation dynamics among financial assets are spurious. The typical correlation dynamics that can be observed in the data are a direct consequence of correlation breaks that occur in response to financial and economic shocks. The presence of breaks affects the correlation parameters *DCC a* and *b*. DCC *a*, which measures the response to shocks, and the parameter *DCC b*, which measures the persistence of correlations, interact in a nonlinear way to generate the correlation dynamics that we usually observe for financial assets. Once these breaks are controlled for, the parameters driving the correlation dynamics change in important ways. A number of parameters are now close to zero and generate constant correlations. The average estimate of *DCC b* which is upward biased in the presence of correlation breaks decreases in subsamples. The sum of *a* and *b* which is usually found to be close to one is therefore lower. These subtle changes remove the parameters from an area of influence that generate typical correlation dynamics. The variance and autocovariance estimates are now lower, indicating that correlation estimates fluctuate at low volatility around a straight line. The true nature of correlations is therefore likely to be constant. The implication for empirical correlation estimates is that the path generated by multivariate GARCH correlations should be interpreted with caution. A portfolio spanning the main asset classes is shown to respond to the way correlations are estimated. A significant break in the correlation structure can distort DCC correlations and lead to a higher portfolio variance. We show that investors can resort to simple solutions such as a rolling window estimator when updating their portfolio weights.

In summary, our results provide a rationale for the often controversial discussion of the value added of dynamic conditional correlation models. A number of dynamic correlation models have formed the basis for a significant amount of important research and we do not propose to reject these models entirely. However, academics and practitioner should be aware of the practical limitations of these models that arise in many finance applications.

Appendix A: Empirical Results for Other Popular MGARCH Models

In this paper we focus on Engle's DCC model which appears to be the most popular and most widely used MGARCH model in empirical research. In the following, we will show that our findings are not confined to the DCC specification but also extend to other more complex MGARCH models. In particular, we find that correlation breaks have similar implications for the coefficient estimates of the diagonal VECH model (Bollerslev, Engle, and Wooldridge, 1988), the BEKK model (Engle and Kroner, 1995), and the corrected DCC model (Aielli, 2013). While differences in model specifications prevent a direct comparison between models, we can observe a distinct change in coefficient estimates across all models.

The diagonal VECH model of Bollerslev, Engle, and Wooldridge (1988) is a restricted version of the more general VECH model and is expressed as

$$H_t = \Omega + A \odot \varepsilon_{t-1}\varepsilon'_{t-1} + B \odot H_{t-1}, \tag{A.1}$$

where the parameter matrices *A* and *B* are indefinite matrices, i.e. the parameters can vary without any restrictions. While this specification does not ensure that the conditional covariance matrix is positive semidefinite, it is also the most general way of writing the diagonal VECH model.

The diagonal BEKK model of Engle and Kroner (1995) is defined as

$$H_t = \Omega\Omega' + A\varepsilon_{t-1}\varepsilon'_{t-1}A' + BH_{t-1}B'. \tag{A.2}$$

The general form of the BEKK model in which *A* and *B* are unrestricted contains many parameters and is computationally expensive. We therefore use the more common diagonal form in which *A* and *B* are restricted to be diagonal matrices.

Aielli (2013) shows that the constant $\vartheta_{i,j}$ in $\hat{q}_{i,j,t} = (1-a-b)\vartheta_{i,j} + ae_{i,t-1}e_{j,t-1} + b\hat{q}_{i,j,t-1}$ can be inconsistent. The constant $\vartheta_{i,j}$ is thought of as the second moment of e_t or $\vartheta = E(e_t e'_t)$. For certain parameter values and large systems containing many assets, this may not be the case which can cause the DCC estimator to be biased. However, Aielli also shows that for parameter values that are common for financial applications the bias is negligible. The correction proposed by Aielli (2013) is

$$\hat{q}_{i,j,t} = (1-a-b)\vartheta_{i,j} + a \cdot \hat{q}_{i,j,t} \cdot e_{i,t-1} e_{j,t-1} + b\hat{q}_{i,j,t-1}. \tag{A.3}$$

We estimate the three models for all assets in our data set. The dynamic correlations produced by the models are very similar. For instance, Figure A1 shows the daily dynamic correlations between the S&P 500 and the NASDAQ composite index. The upper graph is based on the DCC model and is the same as Figure 1 shown in the introduction. The lower graph shows the deviations of the DCC model from the corrected DCC (cDCC), the diagonal VECH, and the diagonal BEKK model. As can be seen, the differences are quite small, so that we should expect the findings in this paper to hold also for other autoregressive MGARCH specifications.

Figure A1: Model Comparison: Daily Conditional Correlations Between S&P 500 and NASDAQ

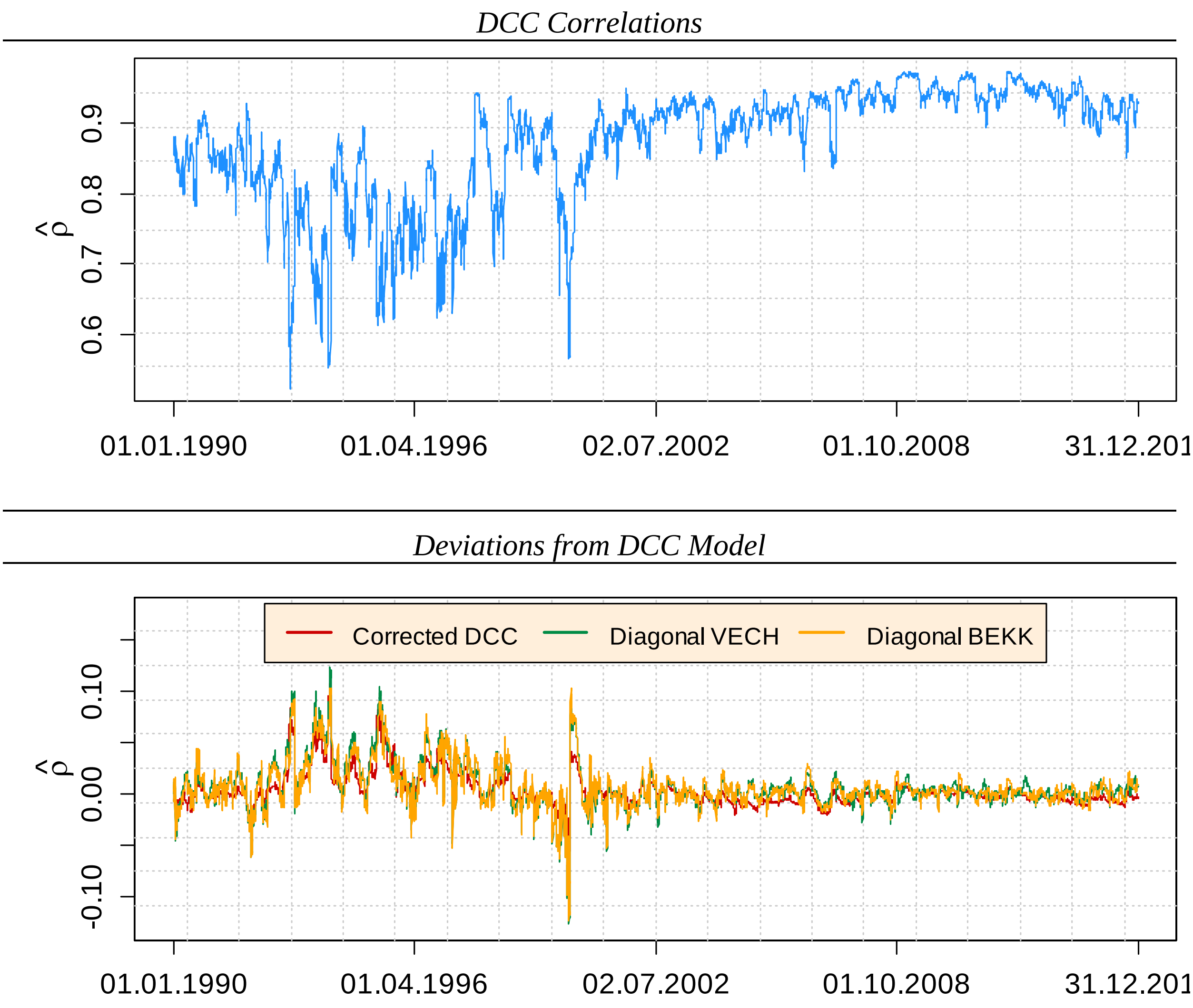

This figure shows typical correlation dynamics generated by a DCC model as well as the deviations from these DCC correlations. The deviations of other popular correlation models are quite small indicating that the results in this paper also extend to other frequently used multivariate GARCH models.

Table A1 repeats the correlation coefficient analysis discussed earlier in Panel A of Figure 4, this time comparing coefficients across different MGARCH models. The first column shows how *DCC a* and *DCC b* parameters change from full samples that contain at least one correlation break to subsamples that occur between breaks. While the ARCH term (in this case the *DCC a* parameter) increases slightly, the GARCH term (in this case the *DCC b* parameter) decreases by 0.134 to 0.836. As we have shown in the paper, this fall is sufficiently large to eliminate most of the variation in $\hat{\rho}_t$. Columns 2 to 4 show a similar decrease in the persistence parameter for the other three models. The reduction is not as large as in the case of the DCC model but it moves the sum of ARCH and GARCH term away from the 0.99 threshold at which correlation dynamics become very pronounced (Aielli, 2013). From the findings in Table A1 we conclude that typical autoregressive MGARCH specifications respond in a similar way to correlations breaks so that our results based on the DCC model can be also extended to other MGARCH specifications.

Table A1: The Impact of Correlation Breaks across Different MGARCH Models

	DCC	**Corrected DCC**	**VECH**	**BEKK**
		Full Sample		
ARCH term	0.021	0.021	0.025	0.049
GARCH term	0.970	0.970	0.941	0.939
		Subsample		
ARCH term	0.027 (+0.006)	0.025 (+0.004)	0.026 (+0.001)	0.045 (-0.004)
GARCH term	0.836 (-0.134)	0.892 (-0.078)	0.894 (-0.047)	0.909 (-0.03)

This Table shows that the presence of correlation breaks affects the persistence parameter and hence the overall correlation dynamics of four popular MGARCH models in a similar way.

Appendix B: The Scalar $\hat{D}$ for the Test Statistic of Wied, Krämer and Dehling (2012)

We briefly describe the construction of the scalar $\hat{D}$ which is part of the expression in Equation (3). For a general and in-depth treatment we refer to Wied, Krämer, and Dehling (2012, Appendix A.1). Let $\left\{(x_{1,t}, x_{2,t})'\right\}$ be the bivariate time-series with $E\left[(x_{1,t}, x_{2,t})'\right] = 0$. Given is a sample of size *T*. For $i = 1,2$, denote $\overline{x_i} = T^{-1}\sum_{t=1}^{T} x_{i,t}$, $\overline{x_i^2} = T^{-1}\sum_{t=1}^{T} x_{i,t}^2$ and $\hat{\sigma}_{x_i} = \sqrt{\overline{x_i^2} - \overline{x_i}^2}$. Further, denote $\overline{x_1 x_2} = T^{-1}\sum_{t=1}^{T} x_{1,t}x_{2,t}$ and $\hat{\sigma}_{x_1x_2} = \overline{x_1x_2} - \overline{x_1}\cdot\overline{x_2}$. Let $k(\cdot)$ be the Bartlett kernel function. The scalar $\hat{D}$ is then given by

$$\hat{D} = \sqrt{\hat{D}_3 \hat{D}_2 \hat{D}_1 \hat{D}_2{}' \hat{D}_3{}'}\,, \tag{B.1}$$

where

$$\hat{D}_1 = \sum_{t=1}^{T}\sum_{u=1}^{T} k\left(\frac{t-u}{\lfloor \log T \rfloor}\right) V_t V_u{}' \tag{B.2}$$

with $V_t = T^{-1/2}\left(x_{1,t}^2 - \overline{x_1^2}, x_{2,t}^2 - \overline{x_2^2}, x_{1,t} - \overline{x_1}, x_{2,t} - \overline{x_2}, x_{1,t}x_{2,t} - \overline{x_1x_2}\right)'$,

$$\hat{D}_2 = \begin{pmatrix} 1 & 0 & -2\overline{x_1} & 0 & 0 \\ 0 & 1 & 0 & -2\overline{x_1} & 0 \\ 0 & 0 & -\overline{x_2} & -\overline{x_1} & 1 \end{pmatrix}, \tag{B.3}$$

and

$$\hat{D}_3 = \begin{pmatrix} -\frac{1}{2}\frac{\hat{\sigma}_{x_1x_2}}{\hat{\sigma}_{x_2}}\hat{\sigma}_{x_1}^{-3} & -\frac{1}{2}\frac{\hat{\sigma}_{x_1x_2}}{\hat{\sigma}_{x_1}}\hat{\sigma}_{x_2}^{-3} & \frac{1}{\hat{\sigma}_{x_1x_2}} \end{pmatrix}. \tag{B.4}$$

The purpose of the scalar $\hat{D}$ is to appropriately rescale the cumulated sum of empirical correlation coefficients in such a way that convergence of Q_T to the asymptotic null distribution is achieved.

Appendix C: List of Assets

Stocks		Bonds	
Name	**DS Mnemonic**	**Name**	**DS Mnemonic**
S&P500	S&PCOMP	US 10 yr. Gov.	BMUS10Y
TSX	TTOCOMP	CA 10 yr. Gov.	BMCN10Y
MIB	FTSEMIB	IT 10 yr. Gov.	BMIT10Y
OMX Stockholm	SWEDOMX	SE 10 yr. Gov.	BMSD10Y
DAX 30	DAXINDZ	GER 10 yr. Gov.	ABDGVG4
CAC 40	FRCAC40	FR 10 yr. Gov.	BMFR10Y
AEX	AMSTEOE	NL 10 yr. Gov.	BMNL10Y
NIKKEI 225	JAPDOWA	JP 10 yr. Gov.	BMJP10Y
KOSPI	KORCOMP	UK 10 yr. Gov.	BMUK10Y
FTSE100	FTSE100	CH 10 yr. Gov.	BMSW10Y
Commodities		**Currencies**	
Name	**DS Mnemonic**	**Name**	**DS Mnemonic**
Copper	GSICTOT	USD–EUR	USEURSP
Corn	GSCNTOT	USD–JPY	JAPYNUS
Crude Oil	SGCRTOT	USD–CAD	CDNDLUS
Heating Oil	GSHOTOT	USD–KRW	SKORWUS
Natural Gas	GSNGTOT	USD–SEK	SWEDKUS
Gold	GSGCTOT	USD–CHF	SWISFUS
Aluminum	GSIATOT	USD–MXN	MEXPFUS
Sugar	GSSBTOT	USD–GBP	BRITPUS
Cotton	GSCTTOT	USD–NOK	NORGKUS
Cattle	GSLCTOT	USD–BRL	BRAZLUS

This table lists the 40 assets that are used in the paper. All time series are from DataStream. The commodities are S&P GSCI Total Return Indices.

Appendix D: Approximation Accuracy of $Cov(\hat{\boldsymbol{\rho}}_t^*, \hat{\boldsymbol{\rho}}_{t-s}^*)$

To assess whether $Cov(\hat{\rho}_t^*, \hat{\rho}_{t-s}^*)$ is a good approximation for $Cov(\hat{\rho}_t, \hat{\rho}_{t-s})$, we simulate a series of 500,000 innovations following the DGP as defined in Equation (10). We can then generate a series of conditional correlations $\hat{\rho}_t$ from the simulated sample according to Equation (1), where $\hat{\mathbf{q}}_t$ is defined by a rolling window estimator as in Equation (7), an EWMA model as in (8), or by the DCC specification of Equation (9). We can measure for approximation accuracy by using the percentage deviation of the approximation $Cov(\hat{\rho}_t^*, \hat{\rho}_{t-s}^*)$ from the sample value of $Cov(\hat{\rho}_t, \hat{\rho}_{t-s})$.

The parameter of the WMA model is set to $\lambda = 0.94$, which is the daily parameter value proposed by RiskMetrics. The choice of the DCC model parameters is based on the estimated values derived from Engle and Sheppard (2001), Engle (2002), and Engle and Colacito (2006). Table D1 gives an overview of the ML estimates reported in these studies. The parameter a ranges from 0.01 and 0.07, b ranges from 0.91 to 0.98, and on average $1 - a - b$ is about 0.01. We therefore set a equal to 0.02, 0.04, or 0.06, while b is defined as $0.99 - a$. Finally, the window size n of the rolling window estimator is set to 60, 120, and 240.

The simulation results are shown in D.1. For the EWMA model, $Cov(\hat{\rho}_t^*, \hat{\rho}_{t-s}^*)$ tends to overstate $Cov(\hat{\rho}_t, \hat{\rho}_{t-s})$ for $\rho = 0.0$ and 0.3, and understate it for $\rho = 0.6$ and 0.9. For the DCC model, $Cov(\hat{\rho}_t^*, \hat{\rho}_{t-s}^*)$ tends to overstate $Cov(\hat{\rho}_t, \hat{\rho}_{t-s})$, while the opposite appears to be true for the rolling window. Overall, the deviations range from -10.26% to 5.96%.

Table D1: Simulated Values $Cov(\hat{\rho}_t, \hat{\rho}_{t-s})$ versus the Approximation $Cov(\hat{\rho}_t^*, \hat{\rho}_{t-s}^*)$

$\boldsymbol{\rho}$	**EWMA**	**DCC with $\boldsymbol{b = 0.99 - a}$**			**Rolling Window**		
	$\lambda = 0.94$	$a = 0.02$	$a = 0.04$	$a = 0.06$	$n = 60$	$n = 120$	$n = 240$
Panel A: lag s = *0*: $(Cov(\hat{\rho}_t^*, \hat{\rho}_t^*)\ / Cov(\hat{\rho}_t, \hat{\rho}_t) - 1) \cdot 100$							
0.0	4.9943	1.4060	5.5689	5.9551	-1.1186	-0.2574	-1.2697
0.3	1.5494	1.4909	3.7652	3.8787	-2.6126	-0.5663	-0.5497
0.6	-1.3444	0.8873	0.5631	0.2382	-5.1407	-1.8598	-1.9055
0.9	-10.2614	0.0674	-2.4617	-6.0443	-9.1979	-5.4237	-0.6458
Panel B: lag s = *5*: $(Cov(\hat{\rho}_t^*, \hat{\rho}_{t-5}^*)\ / Cov(\hat{\rho}_t, \hat{\rho}_{t-5}) - 1) \cdot 100$							
0.0	4.2139	0.9175	5.0035	4.4564	-0.7880	-0.1607	-1.2761
0.3	0.1484	1.1537	3.0081	2.0319	-2.3207	-0.4636	-0.5311
0.6	-2.0026	0.6319	0.1008	-0.8287	-4.8108	-1.7221	-1.8935
0.9	-10.1639	0.2974	-2.3910	-6.0815	-8.6375	-5.3226	-0.5925
Panel C: lag s = *10*: $(Cov(\hat{\rho}_t^*, \hat{\rho}_{t-10}^*)\ / Cov(\hat{\rho}_t, \hat{\rho}_{t-10}) - 1) \cdot 100$							
0.0	4.0909	0.4415	4.5275	3.7571	-0.4778	-0.0782	-1.2807
0.3	-0.9402	0.9954	2.3103	0.1669	-2.0155	-0.3886	-0.5222
0.6	-2.6713	0.3867	-0.0721	-1.6956	-4.5631	-1.5754	-1.8715
0.9	-10.1972	0.1999	-2.5478	-6.4674	-8.0247	-5.2235	-0.5493

This table shows the percentage deviation of the $\boldsymbol{Cov(\hat{\rho}_t^*, \hat{\rho}_{t-s}^*)}$ approximation from the sample value $\boldsymbol{Cov(\hat{\rho}_t, \hat{\rho}_{t-s})}$, with values for s changing from 0 in Panel A to 5 in Panel B, and finally 10 in Panel C. $\boldsymbol{Cov(\hat{\rho}_t, \hat{\rho}_{t-s})}$ is estimated from conditional correlations generated by applying an EWMA model, a DCC model, and a rolling window estimator to a series of simulated innovations as defined in (10). The true underlying correlation $\boldsymbol{\rho}$ changes over typical values: 0, 0.3, 0.6, and 0.9.

Appendix E. Proof of Proposition 1

We begin with the expressions $(\hat{\mathbf{q}}_t, \hat{\mathbf{q}}_{t-s})$ for the DCC and the EWMA model (labeled *i* and *ii* in Proposition 1). First, let $\mathbf{g}_t = (e_{1,t}^2 \quad e_{2,t}^2 \quad e_{1,t}e_{2,t})'$ so that $\mathrm{E}(\mathbf{g}_t) = \boldsymbol{\varphi} = (1, 1, \rho)'$ and

$$\hat{\mathbf{q}}_t = (1-a-b)\boldsymbol{\varphi} + a\mathbf{g}_{t-1} + b\hat{\mathbf{q}}_{t-1}, \tag{E.1}$$

with $0 < a < 1$, $0 < b < 1$ and $a + b < 1$. Defining $\mathbf{u}_t = a(\mathbf{g}_{t-1} - \boldsymbol{\varphi})$ such that $\mathrm{E}(\mathbf{u}_t) = 0$ and $\mathbf{B} = b\mathbf{I}$, we can rewrite (E.1) as a VAR(1) process:

$$\begin{aligned}\hat{\mathbf{q}}_t &= (1-b)\boldsymbol{\varphi} + \mathbf{B}\hat{\mathbf{q}}_{t-1} + \mathbf{u}_t,\\ &= (1-b)\boldsymbol{\varphi}\lim_{\mathrm{i}\to\infty}\left(\mathbf{I} + \mathbf{B} + \cdots + \mathbf{B}^{\mathrm{i}}\right) + \textstyle\sum_{\mathbf{s}=\mathbf{0}}^{\infty}\mathbf{B}^{\mathbf{s}}\mathbf{u}_{t-s},\\ &= \boldsymbol{\varphi} + \textstyle\sum_{\mathbf{s}=\mathbf{0}}^{\infty}\mathbf{B}^{\mathbf{s}}\mathbf{u}_{t-s},\end{aligned} \tag{E.2}$$

where we use the fact that $\lim_{\mathrm{i}\to\infty}\left(\mathbf{I} + \mathbf{B} + \cdots + \mathbf{B}^{\mathrm{i}}\right) = \frac{1}{1-\mathrm{b}}\mathbf{I}$. Equation (E.2) is stationary if all eigenvalues of $\mathbf{B}$ are less than 1 in absolute values, which is satisfied here as we assume $0 < b < 1$ (this is a common assumption, see e.g. Lütkepohl, 2006). Because $\hat{\mathbf{q}}_t$ is stationary, $E(\mathbf{u}_t\mathbf{u}'_{t-s}) = \mathbf{0}$ and $E(\mathbf{u}_t\mathbf{u}'_t) = \boldsymbol{\Sigma}_\mathbf{u}$ for all *t*. Also, $\boldsymbol{\Sigma}_\mathbf{u}$ is invertible for $|\rho| < 1$. It follows that

$$Cov(\hat{\mathbf{q}}_t, \hat{\mathbf{q}}_{t-s}) = \textstyle\sum_{\mathbf{i}=\mathbf{0}}^{\infty}\mathbf{B}^{\mathbf{s}+\mathbf{i}}\boldsymbol{\Sigma}_\mathbf{u}(\mathbf{B}^{\mathbf{i}})'. \tag{E.3}$$

Hence, all that is needed to get $Cov(\hat{\mathbf{q}}_t, \hat{\mathbf{q}}_{t-s})$ is $E(\mathbf{u}_t\mathbf{u}'_t)$. Denoting $\boldsymbol{\varphi}\boldsymbol{\varphi}' = \boldsymbol{\Lambda}$ and $E(\mathbf{g}_t\mathbf{g}'_t) = \boldsymbol{\Gamma}$, we can write $\boldsymbol{\Sigma}_\mathbf{u} = a^2(\boldsymbol{\Gamma} - \boldsymbol{\Lambda})$ and therefore

$$Cov(\hat{\mathbf{q}}_t, \hat{\mathbf{q}}_{t-s}) = \textstyle\sum_{\mathrm{i}=0}^{\infty}\mathbf{B}^{\mathbf{s}+\mathbf{i}}a^2(\boldsymbol{\Gamma} - \boldsymbol{\Lambda})(\mathbf{B}^{\mathbf{i}})' = a^2(\boldsymbol{\Gamma} - \boldsymbol{\Lambda})\frac{b^s}{1-b^2}. \tag{E.4}$$

Because $\boldsymbol{\Omega} = \boldsymbol{\Gamma} - \boldsymbol{\Lambda}$, Equation (E.4) implies the DCC case *(i)* for $(a+b) < 1$ and the EWMA case *(ii)* for $0 < \lambda = b = (1-a) < 1$.

Next, we turn to the expression $(\hat{\mathbf{q}}_t, \hat{\mathbf{q}}_{t-s})$ for the rolling window estimator (labeled *iii* in Proposition 1). Let again $\mathbf{g}_t = (e_{1,t}^2 \quad e_{2,t}^2 \quad e_{1,t}e_{2,t})'$, $\mathrm{E}(\mathbf{g}_t) = \boldsymbol{\varphi} = (1, 1, \rho)'$, $\boldsymbol{\varphi}\boldsymbol{\varphi}' = \boldsymbol{\Lambda}$ and $E(\mathbf{g}_t\mathbf{g}'_t) = \boldsymbol{\Gamma}$. Because $Cov(\hat{\mathbf{q}}_t, \hat{\mathbf{q}}_{t-s}) = E(\hat{\mathbf{q}}_t\hat{\mathbf{q}}'_{t-s}) - \boldsymbol{\Lambda}$ we have to derive $E(\hat{\mathbf{q}}_t\hat{\mathbf{q}}'_{t-s})$ for all $s \geq 0$. For the rolling window estimator, we rewrite $\hat{\mathbf{q}}_t$ as $\hat{\mathbf{q}}_t = \frac{1}{n}\sum_{l=1}^{n} \mathbf{g}_{t-l}$. First, let $s = 0$. In this case

$$E(\hat{\mathbf{q}}_t\hat{\mathbf{q}}'_t) = \frac{1}{n^2}\sum_{\mathrm{k}=1}^{\mathrm{n}}\sum_{\mathrm{l}=1}^{\mathrm{n}} E\left(\mathbf{g}_{t-l}\mathbf{g}'_{t-k}\right),$$

$$= \frac{1}{n^2}(n\mathbf{\Gamma} + \mathrm{n}(\mathrm{n}-1)\mathbf{\Lambda}), \tag{E.5}$$

$$= \frac{n}{n^2}(\mathbf{\Gamma} - \mathbf{\Lambda}) + \mathbf{\Lambda}.$$

Next consider $0 < s = n$. Note that we can write $\hat{\mathbf{q}}_{t-s} = \hat{\mathbf{q}}_{t-(s-1)} - \frac{1}{n}\left(\mathbf{g}_{t-s}\mathbf{g}'_{t-s-n}\right)$ such that

$$E(\hat{\mathbf{q}}_t\hat{\mathbf{q}}'_{t-s}) = E\left(\hat{\mathbf{q}}_t\hat{\mathbf{q}}'_{t-(s-1)}\right) - \frac{1}{n}\left(E\left(\hat{\mathbf{q}}_t\mathbf{g}'_{t-s}\right) - E\left(\hat{\mathbf{q}}_t\mathbf{g}'_{t-s-n}\right)\right),$$

$$= E\left(\hat{\mathbf{q}}_t\hat{\mathbf{q}}'_{t-(s-1)}\right) - \frac{1}{n}\left(\frac{1}{n}\mathbf{\Gamma} + \frac{\mathrm{n}-1}{\mathrm{n}}\mathbf{\Lambda} - \mathbf{\Lambda}\right), \tag{E.6}$$

$$= E\left(\hat{\mathbf{q}}_t\hat{\mathbf{q}}'_{t-(s-1)}\right) - \frac{1}{n^2}(\mathbf{\Gamma} - \mathbf{\Lambda}).$$

Substituting $\frac{\mathrm{n}-(\mathrm{s}-1)}{\mathrm{n}^2}(\mathbf{\Gamma} - \mathbf{\Lambda}) + \mathbf{\Lambda}$ for $E\left(\hat{\mathbf{q}}_t\hat{\mathbf{q}}'_{t-(s-1)}\right)$ in (E.6) yields $E(\hat{\mathbf{q}}_t\hat{\mathbf{q}}'_{t-s}) - \frac{n-s}{n^2}(\mathbf{\Gamma} - \mathbf{\Lambda}) + \mathbf{\Lambda}$. Recalling $Cov(\hat{\mathbf{q}}_t, \hat{\mathbf{q}}_{t-s}) = E(\hat{\mathbf{q}}_t\hat{\mathbf{q}}'_{t-s}) - \mathbf{\Lambda}$ and $\mathbf{\Omega} = \mathbf{\Gamma} - \mathbf{\Lambda}$, (E.5) and (E.6) thus imply $Cov(\hat{\mathbf{q}}_t, \hat{\mathbf{q}}_{t-s}) = \frac{\mathrm{n}-\mathrm{s}}{\mathrm{n}^2}\mathbf{\Omega}$ for $0 \leq s < n$. Obviously, for all $s \geq n$ we have $E(\hat{\mathbf{q}}_t\hat{\mathbf{q}}'_{t-s}) = \mathbf{\Lambda}$ so $Cov(\hat{\mathbf{q}}_t, \hat{\mathbf{q}}_{t-s})$ is the null matrix. Hence, the proof is complete.

References

Adrian, T., and M. Brunnermeier (2016): CoVaR. *American Economic Review*, forthcoming

Aielli, G. (2013): Dynamic conditional correlation: On properties and estimation. *Journal of Business and Economic Statistics* 31(3), 282–299.

Andreou, E., and E. Ghysels (2002): Detecting Multiple Breaks in Financial Market Volatility Dynamics. *Journal of Applied Econometrics* 17(5), 579–600.

Andreou, E., and E. Ghysels (2003): Tests for breaks in the conditional co-movement of asset returns. *StatisticaSinica* 13(4), 1045–1073.

Bauwens, L., S. Laurent, and J. Rombouts (2006): Multivariate GARCH models: A survey. *Journal of Applied Econometrics* 21(1), 79–109.

Bera, A., and S. Kim (2002): Testing constancy of correlation and other specifications of the BGARCH model with an application to international equity returns. *Journal of Empirical Finance* 9(2), 171–195.

Bollerslev, T. (1990): Modelling the coherence in short-run nominal exchange rates: A multivariate generalized ARCH model. *Review of Economics and Statistics* 72(3), 498–505.

Bollerslev, T., R. Engle, and Wooldridge (1988): A Capital Asset Pricing Model with Time-varying Covariances. *Journal of Political Economy* 96(1), 116–131.

Bollerslev, T., R. Chou, and K. Kroner (1992): ARCH modeling in finance: A review of theory and empirical evidence. *Journal of Econometrics* 52(1–2), 5–59.

Brenner, M., R. Pasquariello, and M. Subrahmanyam (2009): On the volatility and comovement of U.S. financial markets around macroeconomic news announcements. *Journal of Financial and Quantitative Analysis* 44(6), 1265–1289.

Cai, Y., R.Y. Chou, and D. Li (2009): Explaining International Stock Correlations with CPI Fluctuations and Market Volatility. *Journal of Banking and Finance* 33(11), 2026–2035.

Campbell, J.W., A.W. Lo, and C. MacKinley (1997): The Econometrics of Financial Markets. Princeton University Press.

Caporin, M., and M. McAleer (2012): Do we really need both BEKK and DCC? A tale of two multivariate GARCH models. *Journal of Economic Surveys* 26(4), 736–751.

Cappiello, L., R.F. Engle, and K. Sheppard (2006): Asymmetric Dynamics in the Correlations of Global Equity and Bond Returns. *Journal of Financial Econometrics* 4(4), 537–572.

Chang, C., M. McAleer, and R. Tansuchat (2011): Crude oil hedging strategies using dynamic multivariate GARCH. *Energy Economics* 22(5), 912–923.

Christiansen, C. (2000): Macroeconomic Announcement Effects on the Covariance Structure of Government Bond Returns. *Journal of Empirical Finance* 7(5), 479–507.

Davidson J. (1994): Stochastic Limit Theory: An Introduction for Econometricians. Oxford University Press.

Davis, R.B. (1977): Hypothesis Testing When a Nuisance Parameter is Present only Under the Alternative, *Biometrica*, 64, 247–254.

DeMiquel, V., L. Garlappi, and R. Uppal (2009): Optimal versus naïve diversification: How inefficient is the 1/N portfolio strategy? Review of Financial Studies, 22(5), 1915-1953.

Engle, R. (2002): Dynamic Conditional Correlation – A simple class of multivariate GARCH models. *Journal of Business and Economic Statistics* 20(3), 339–350.

Engle, R., and R. Colacito (2006): Testing and valuing dynamic correlations for asset allocation. *Journal of Business and Economic Statistics* 24(2), 238–253.

Engle, R., C. Granger, and D. Kraft (1984): Combining competing forecasts of inflation based on a multivariate ARCH model. *Journal of Economic Dynamics and Control* 8(2), 151–165.

Engle, R., and K. Kroner (1995): Multivariate simultaneous generalized ARCH. *Econometric Theory* 11(1), 122–150.

Engle, R., and V. Ng (1993): Measuring and Testing the Impact of News on Volatility. *Journal of Finance*, 48(5), 1749–1778.

Engle, R., and K. Sheppard (2001): Theoretical and empirical properties of dynamic conditional correlation multivariate GARCH. NBER Working Papers 8554, National Bureau of Economic Research.

Forbes, K.J., and R. Rigobon (2002): No Contagion, Only Interdependence: Measuring Stock Market Comovements. *The Journal of Finance* 57, 2223–2261.

Foster, D., and D. Nelson (1996): Continuous record asymptotics for rolling sample variance estimators. *Econometrica*, 64(1), 139–174.

Fleming, K., C. Kirby, and B. Ostdiek (2001): The Economic Value of Volatility Timing. *Journal of Finance* 56(1), 329–352.

Galeano, P., and D. Wied (2014): Multiple break detection in the correlation structure of random variables. *Computational Statistics and Data Analysis*, 76, 262–282.

Hamilton, J. and R. Susmel (1994): Autoregressive Heteroscedasticity and Changes in Regime. *Journal of Econometrics* 64(1), 307–333.

Heaney, R. and S. Sriananthakumar (2012): Time-varying correlation between stock market returns and real estate returns. *Journal of Empirical Finance* 19(4), 583–594.

Hillebrand, E. (2005): Neglecting Parameter Changes in GARCH Models. *Journal of Econometrics*, 129(1), 121–138.

Inclán, C., and G.C. Tiao (1994): Use of Cumulative Sums of Squares for Retrospective Detection of Changes in Variance. *Journal of the American Statistics Association* 89, 913–923.

Karolyi, A., and R. Stulz (1996): Why do markets move together? An investigation of U.S.-Japan stock return comovements. *Journal of Finance*, 51 (3), 951–986.

King, M., E. Sentana, and S. Wadhwani (1994): Volatility and links between national stock markets. *Econometrica* 62(4), 901–933.

Kroner, K., and V. Ng (1998): Modeling asymmetric comovements of asset returns. *Review of Financial Studies* 11(4), 817–844.

Kwan, C. (2008): Estimation error in the average correlation of security returns and shrinkage estimation of covariance and correlation matrices. *Finance Research Letters* 5(4), 236–244.

Longerstaey, J., and L. More (1995): Introduction to RiskMetricsTM, 4th e. Morgan Guaranty Trust Company, New York.

Longin, F., and B. Solnik (1995): Is the correlation in international equity returns constant: 1960–1990? *Journal of International Money and Finance* 14(1), 3–26.

Lütkepohl, H. (2006): New introduction to multiple time series analysis. Springer Berlin Heidelberg.

Mittnik, S., and M.S. Paolella (2000): Conditional Density and Value-at-Risk Prediction of Asian Currency Exchange Rates. *Journal of Forecasting* 19(4), 313–333.

Moskowitz, T.J. (2003): An Analysis of Covariance Risk and Pricing Anomalies. *Review of Financial Studies* 16(2), 417–457.

Ofek, E., and M. Richardson (2003): DotCom Mania: The Rise and Fall of Internet Stock Prices. *Journal of Finance* 58(3), 1113–1138.

Pelletier, D. (2006): Regime-switching for Dynamic Correlations. *Journal of Econometrics* 131(1–2), 445–473.

Pérignon, C., and D. Smith (2010): Diversification and Value-at-Risk. *Journal of Banking and Finance* 34(1), 55–66.

Pukthuanthong, K. and R. Roll (2011): Gold and the dollar (and the Euro, Pound, and Yen). *Journal of Banking and Finance* 35(8), 2070–2083.

Quandt, R. (1960): Tests of the Hypothesis that a Linear Regression System obeys two separate regimes. *Journal of the American Statistical Association* 55, 324–330.

Rapach D., and J. Strauss (2008): Structural breaks and GARCH models exchange rate volatility, Journal of Applied Econometrics, 23(1), 65–90.

Sadorsky, P. (2012): Correlations and volatility spillovers between oil prices and the stock prices of clean energy and technology companies. *Energy Economics* 34(1), 248–255.

Tang, G.Y.N. (1995): Intertemporal Stability in International Stock Market Relationships: A Revisit. *The Quarterly Review of Economics and Finance*, 35(1), 579–593.

Tse, Y., and A. Tsui (1999): A note on diagnosing multivariate conditional heteroscedasticity models. *Journal of Time Series Analysis* 20(6), 679–691.

Tse, Y. (2000): A test for constant correlations in a multivariate GARCH model. *Journal of Econometrics* 98(2), 107–127.

You, L., and R. Daigler (2010): Is international diversification really beneficial? *Journal of Banking and Finance* 34(1), 163–173.

West, K.D., and D. Cho (1995): The Predictive Ability of Several Models of Exchange Rate Volatility. *Journal of Econometrics* 69(2), 367–391.

Wied, D., W. Krämer, and H. Dehling (2012): Testing for a Change in Correlation at an Unknown Point in Time Using an Extended Functional Delta Method. *Econometric Theory* 28(3), 1–20.

Figure 1: Daily Conditional Correlations between S&P 500 and NASDAQ Returns

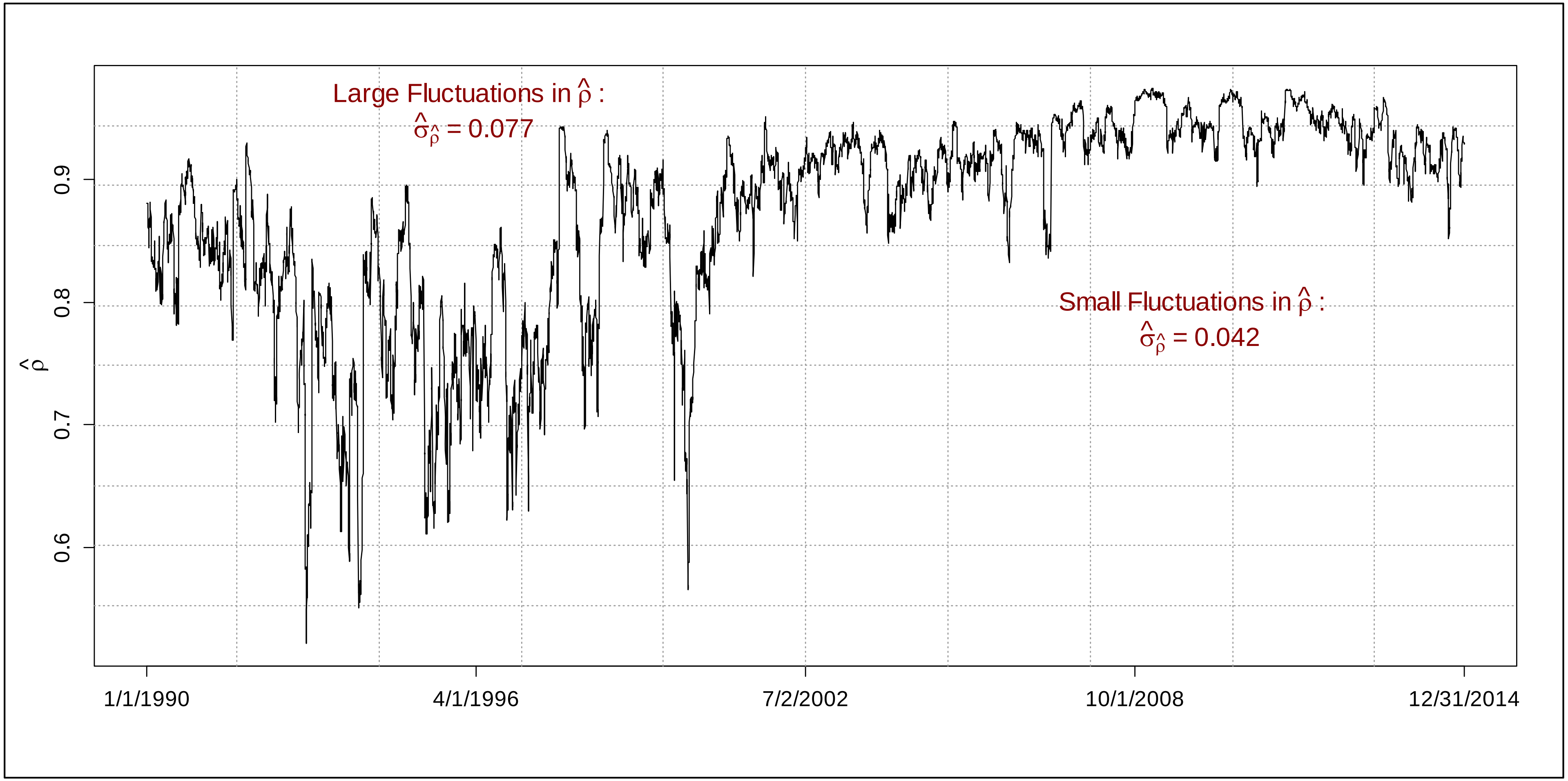

This figure shows daily DCC correlations between the S&P500 Composite index and the NASDAQ Composite index from 01/01/1990 to 12/31/2014 (6,532 obs.). The figure shows that the fluctuations in time-varying correlations is generally high and can change substantially over time. During the period from January 1990 to March 2000 the volatility of daily correlations was 0.077 (122% on an annualized basis) but decreased in the following period (March 2000 to December 2014) to 0.042 (66% annualized).

Figure 2: Are Daily Conditional Correlations between S&P 500 and NASDAQ Returns Constant?

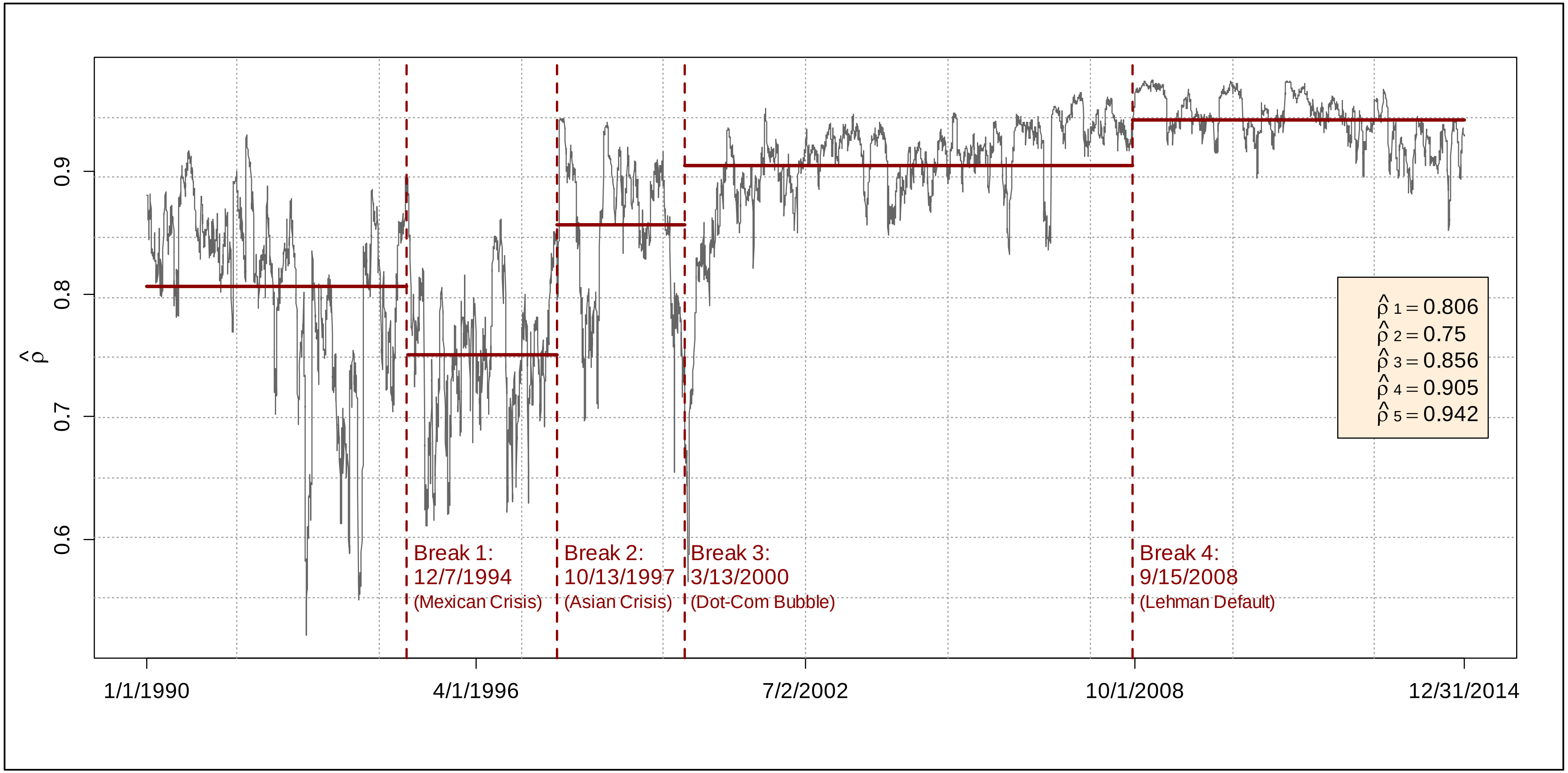

This figure shows the decomposition of daily dynamic correlations into constant correlations that are separated by level shifts. The level shifts are detected by the correlation breakpoint test proposed by Wied, Krämer, and Dehling (2012). The identified breaks are associated with significant disruptions in financial markets such as the burst of the Dot-com bubble in March 2000 or the failure of Lehman Brothers in September 2008.

Figure 3: Correlation Breaks: Descriptive Statistics

Panel A: Distribution of Correlation Breaks Over Time

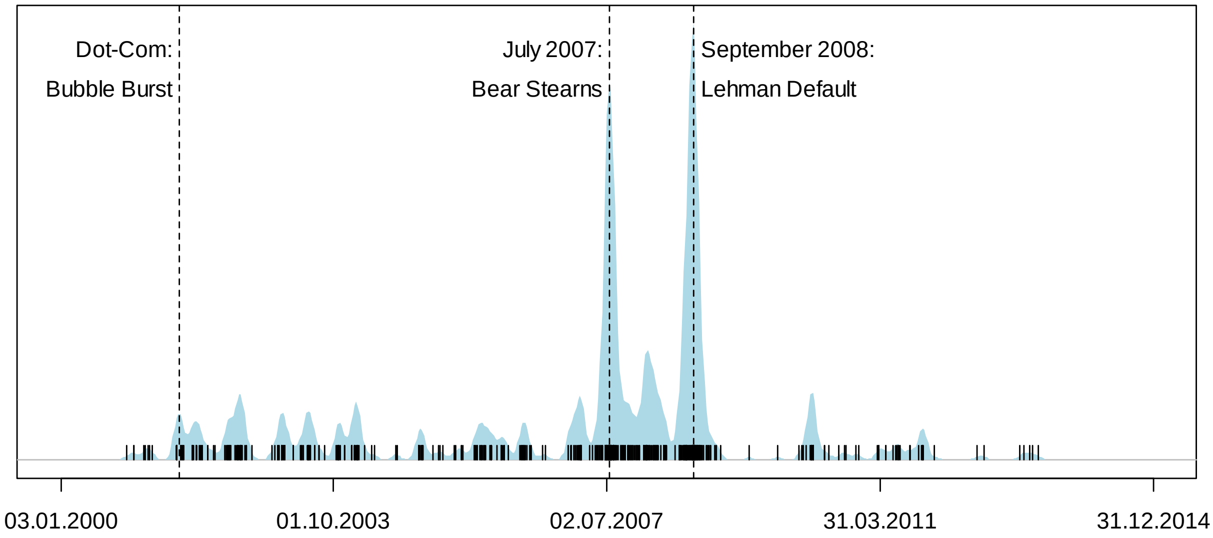

Panel B: Number of Correlation Breaks (2000 – 2014)

0	**1**	**2**	**3**	**4**	**5**
201 (26%)	420 (54%)	84 (10%)	47 (6%)	16 (2%)	6 (1%)

Panel C: Change in Average Correlation $\hat{\rho}$ Following a Break

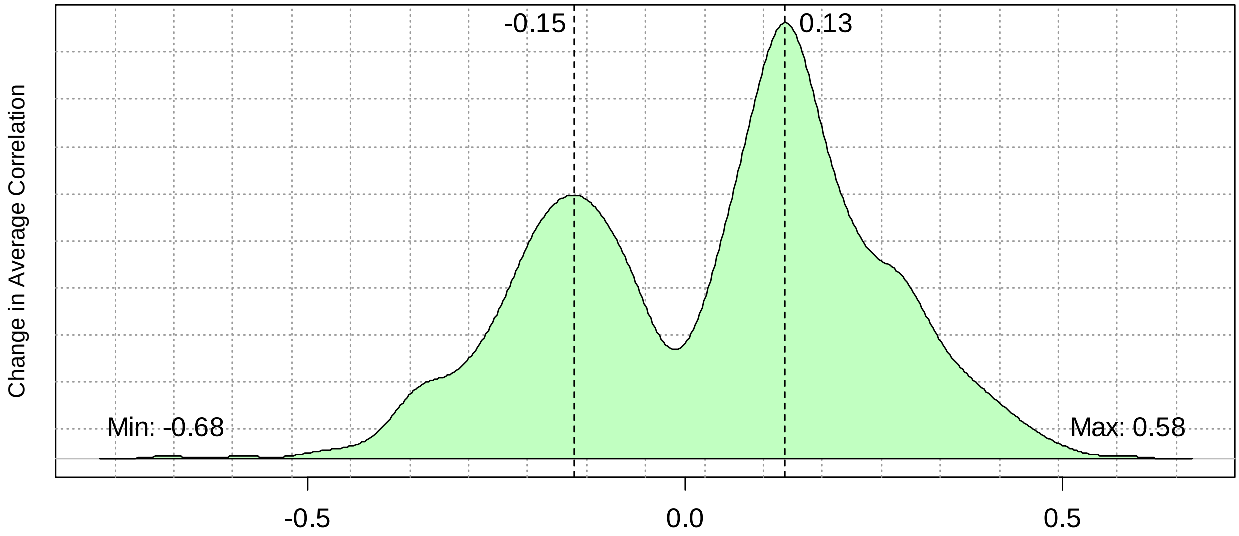

This figure shows the distribution of correlation breaks over time (Panel A), the frequency of breaks (Panel B), and the average change in correlations following a break (Panel C). Breaks are estimated over 40 assets including stocks, bonds, commodities, and currencies for a total of $(40 \cdot 39)/2 = 780$ correlation pairs. The WKD test detects 775 breaks in daily correlations over the period 2000 to 2014.

Figure 4: DCC Parameters in Full Samples and Subsamples

Panel A: Descriptive Statistics of DCC Parameters

	Mean	SD	Min	Max	Significant
			Full Sample		
DCC a	0.021	0.010	0.010	0.059	91%
DCC b	0.970	0.018	0.847	0.988	100%
			Subsample		
DCC a	0.027	0.023	0.000	0.244	58%
DCC b	0.836	0.276	0.000	0.997	87%

Panel B: Distribution of DCC Parameters across Assets

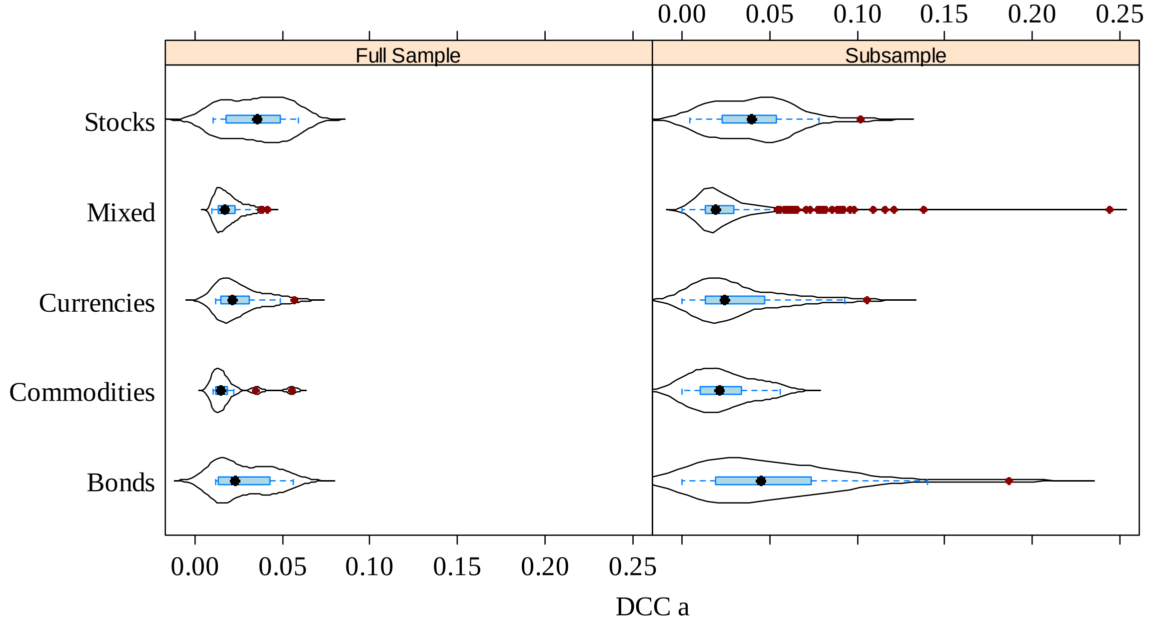

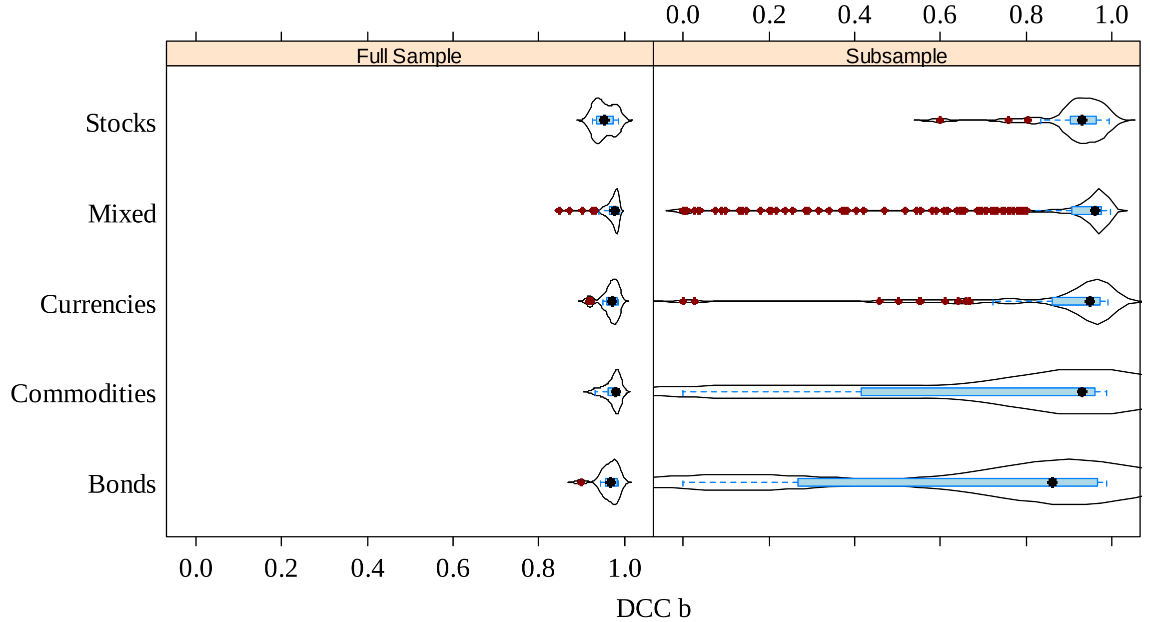

This figure compares the behavior of DCC parameters in full samples and subsamples. The full sample consists of correlations that experience at least one break from 2000 to 2014 (74% of our sample) and have DCC parameters within typical ranges: $0.01 < a < 0.06$ and $0.8 < b < 0.99$ (62% of our sample or 355 correlation series). The parameters in both samples are based on the same asset pairs to allow a direct comparison.

Figure 5: The Parabolic Relationship Between the Level and Volatility of Dynamic Correlations

Panel A: Variation in $\hat{\rho}$ as a Function of the Underlying ρ : Theory and Empirical Evidence

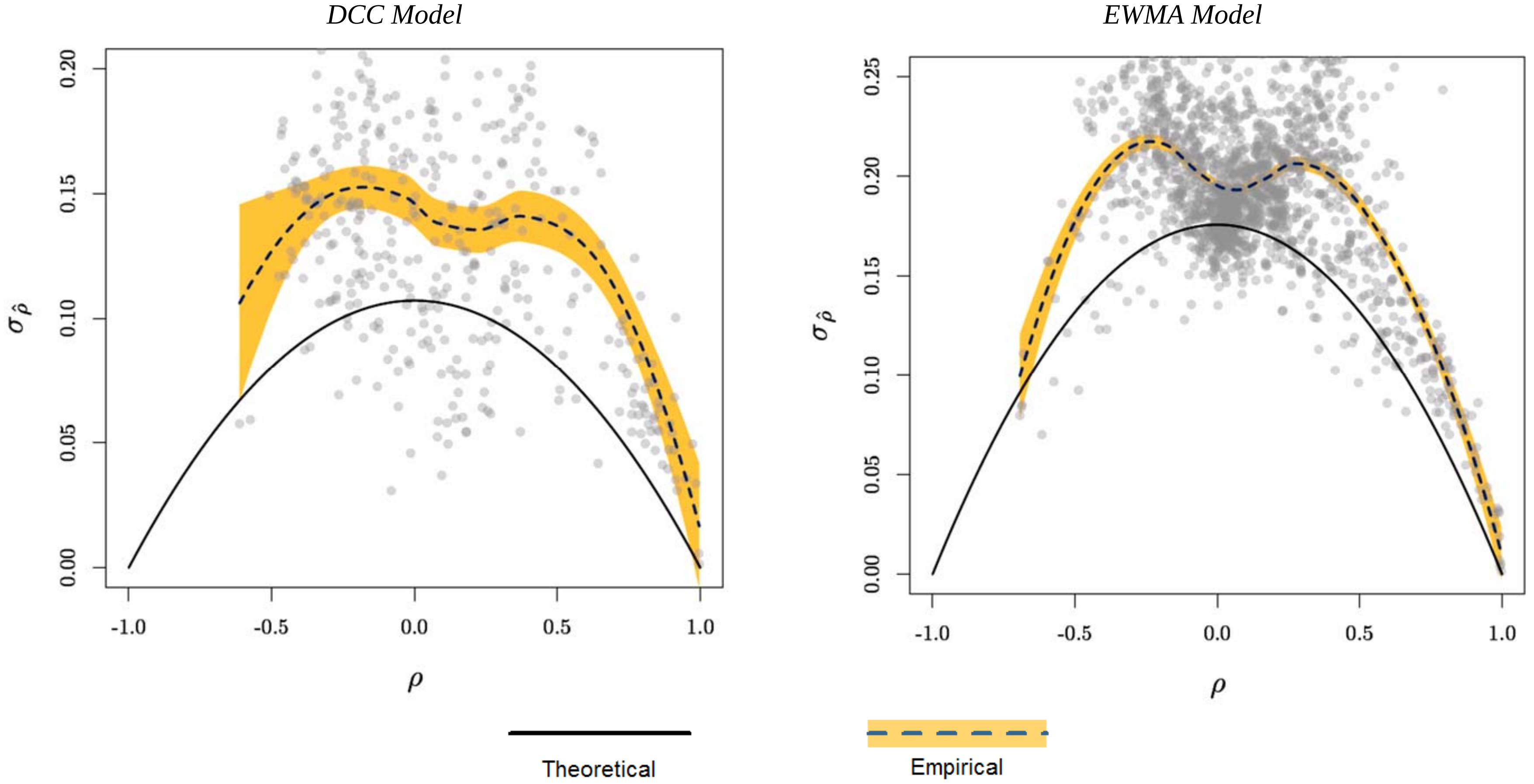

Panel B: Simulated Relationship and the Connection to Volatility: A Comparison

Simulated Relationship with Constant Correlations

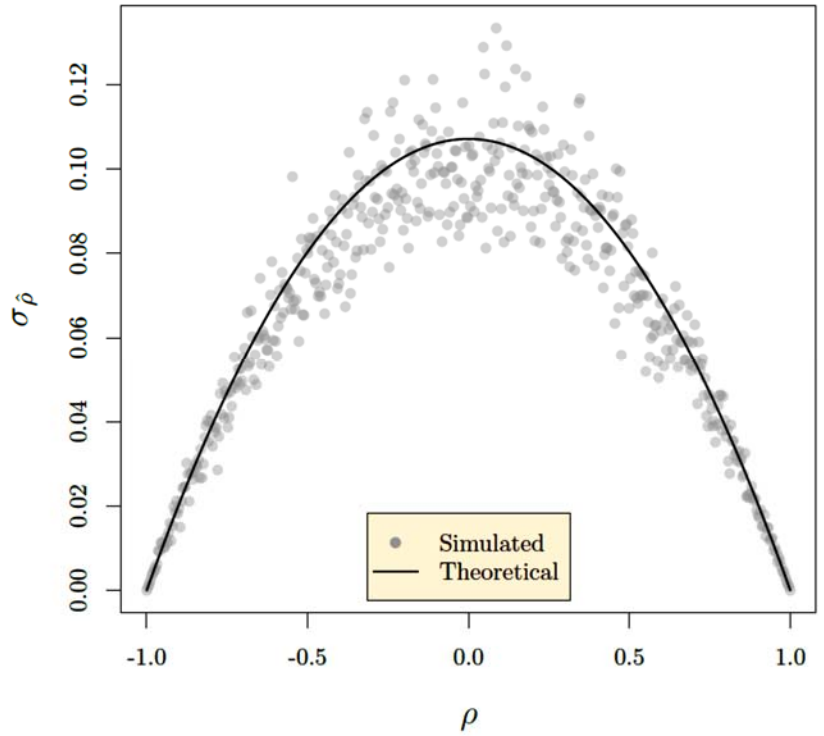

Linear Relationship for Volatilities

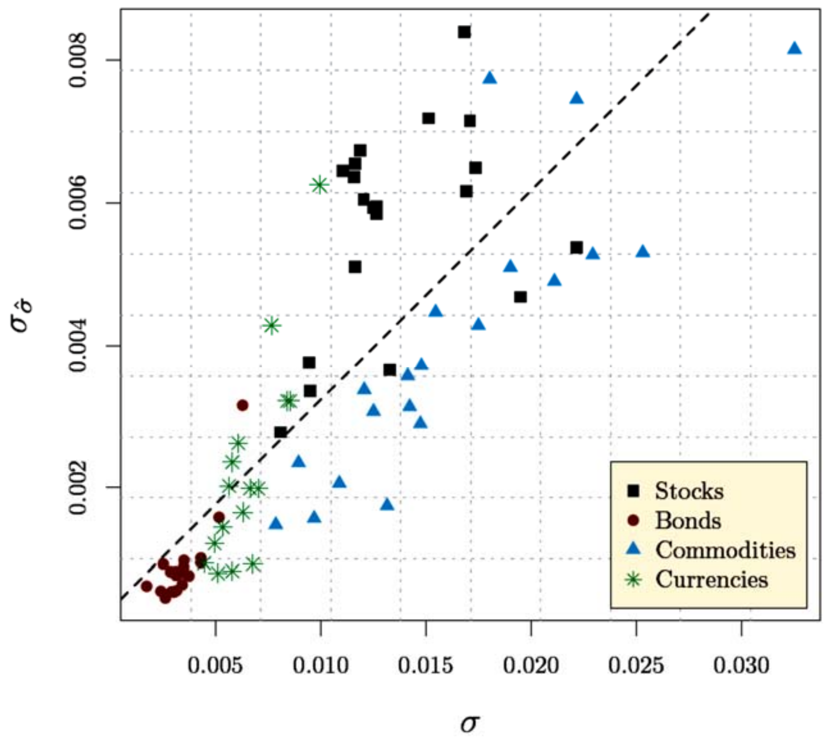

This figure shows how typical estimators of dynamic correlations, $\hat{\rho}$, are influenced by the levels of the true but unobserved correlation ρ. Panel A compares the theoretical behavior, indicated by the inverse parabolic relationship (solid line) with the actual behavior found in the data (dashed line). The theoretical relationship for the DCC model is based on $DCC\ a = 0.03$ and $DCC\ b = 0.96$. The theoretical relationship for the EWMA model is based on $\lambda = 0.94$ and $1-\lambda = 0.06$. The data consists of various correlation pairs from common indices representing stocks, bonds, commodities, and currencies. The points in the left graph show the means and standard deviations of 404 DCC correlations from this group of assets. The right graph shows the estimates of the EWMA correlations and consists of 1,613 observations. The lower number of observations for the DCC model results from excluding correlations with $DCC\ a$ estimates of less than 0.02 and $DCC\ b$ estimates of less than 0.8. Panel B gives an example of the relationship in a controlled simulated environment and shows the case for univariate volatility models. The left graph shows the simulated relationship between variation and level of ρ when the true underlying ρ is constant over time. The right graph shows that the pronounced relationship between the level and volatility of ρ is unique to dynamic correlation models and does not extend to univariate GARCH models.

Figure 6: Estimates of DCC a and b are Different in Subsamples

Panel A: *DCC a* and *b* Estimates in Full Samples and Subsamples

Full Sample | **Subsample**

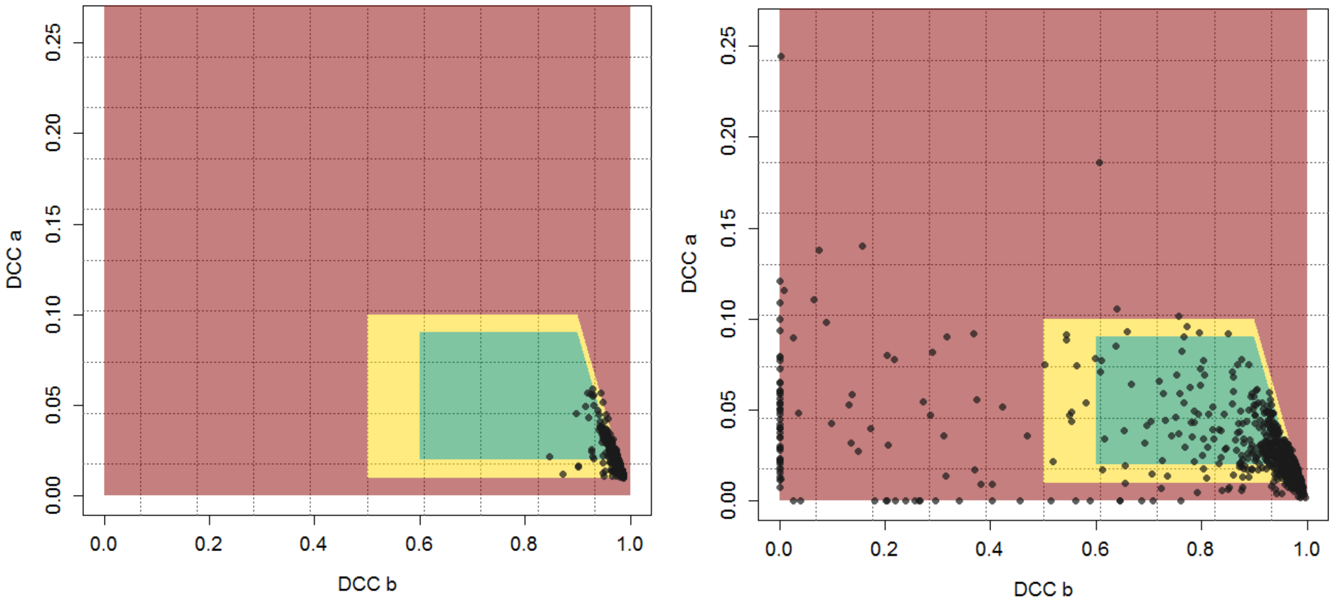

Panel B: Examples: The Impact of Low DCC Parameter Values on Correlation Dynamics

Impact of low *DCC a* | **Impact of low *DCC b***

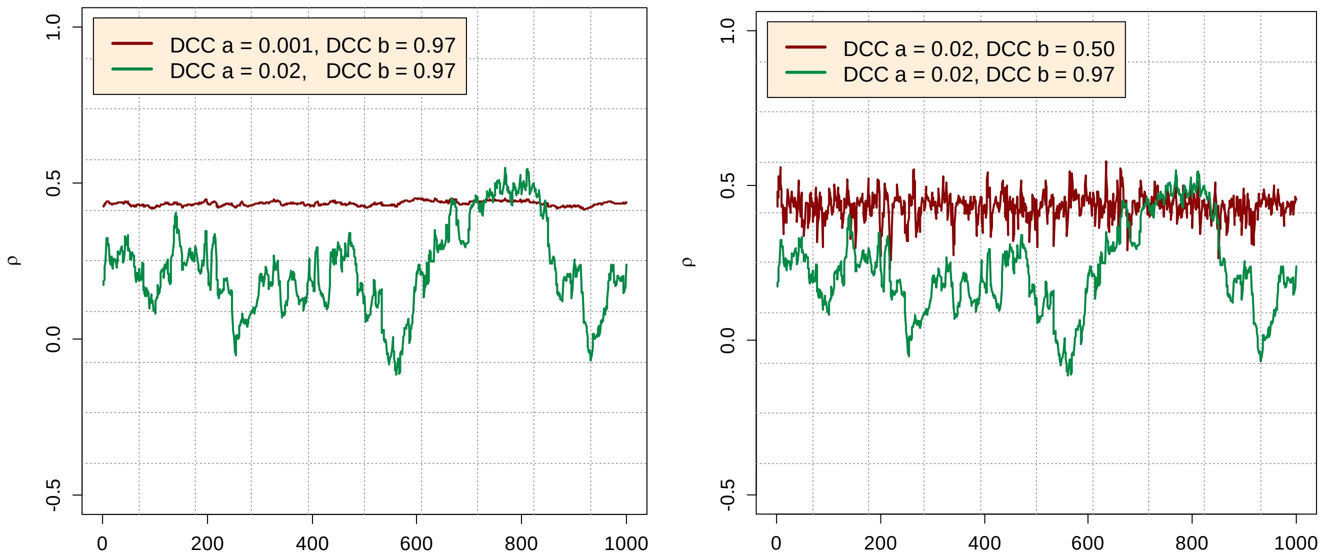

This figure shows the distribution of *DCC a* and *b* parameters in full samples and subsamples. When parameter estimates move outside a narrow range they generate correlations that show little variation over time. For instance, a low *DCC a* value generates near constant correlations. A low *DCC b* value generates correlations that fluctuate at low volatility around a constant value.

Figure 7: The Nonlinear Impact of DCC Parameters on $Var(\hat{\rho})$

Panel A: Subsample DCC Estimates Imply Lower Fluctuations in $\hat{\rho}$

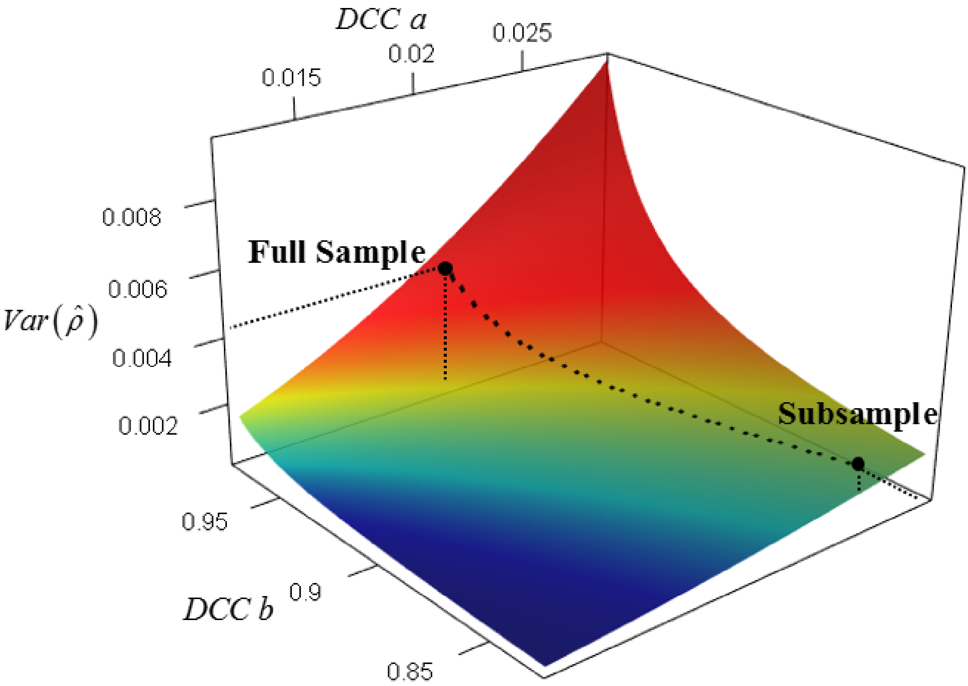

Panel B: Subsample DCC b Values Imply Lower Persistance in $\hat{\rho}$

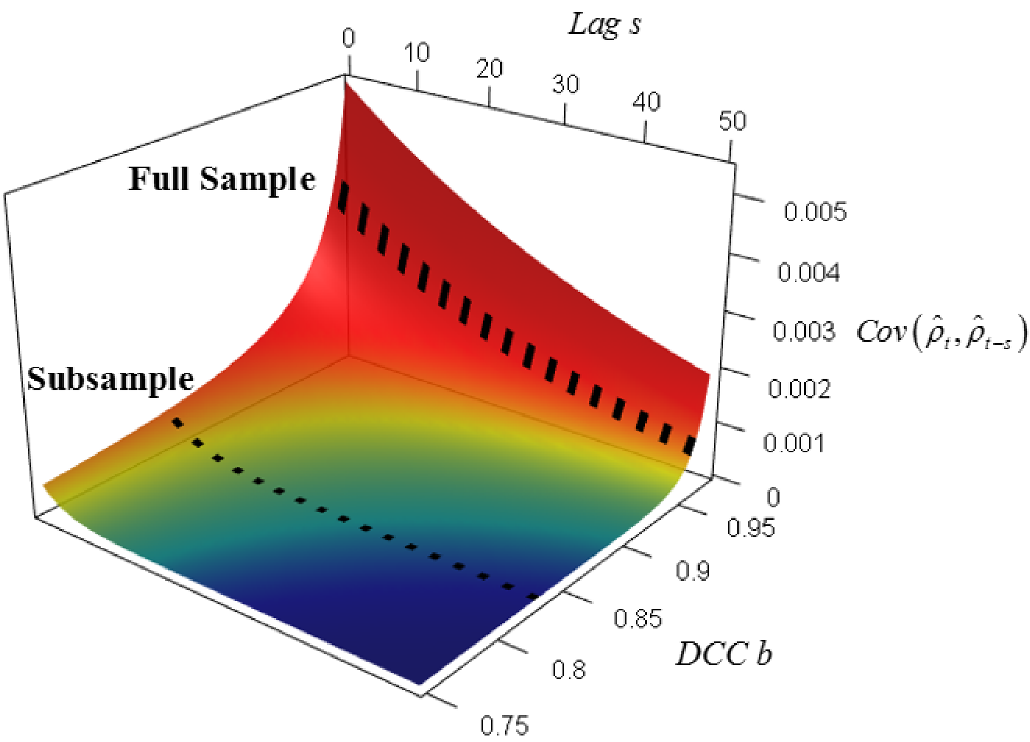

This figure shows that $DCC\ a$ and b values need to lie within a narrow area in order to produce meaningful dynamics in $\hat{\rho}$. The parameter estimates found in subsamples are not sufficiently large to have either significant fluctuations or noticeable autocovariance.

Figure 8: DCC Model Performance in the Asset Portfolios

Panel A: Procedure for Generating Equally Sized Sample Windows

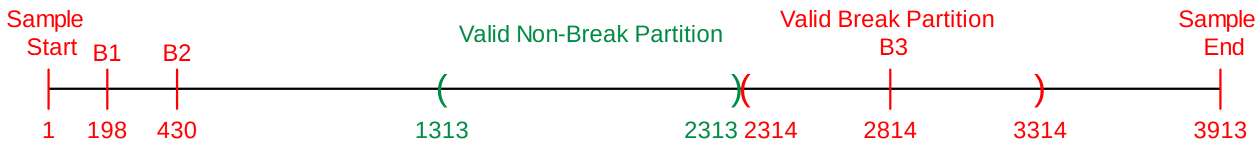

Panel B: Number of Cases When DCC generates the Lowest Portfolio Variance

Expected Returns	Break	Non-Break
[0;1]	62.5%	80.0%
[0.31;0.95]	52.0%	61.3%
[0.59;0.81]	55.5%	60.4%
[0.81;0.59]	61.1%	61.1%
[0.95;0.31]	59.7%	69.2%
[1;0]	60.4%	73.9%

Panel C: DCC Performance Deteriorates for Large Correlation Breaks

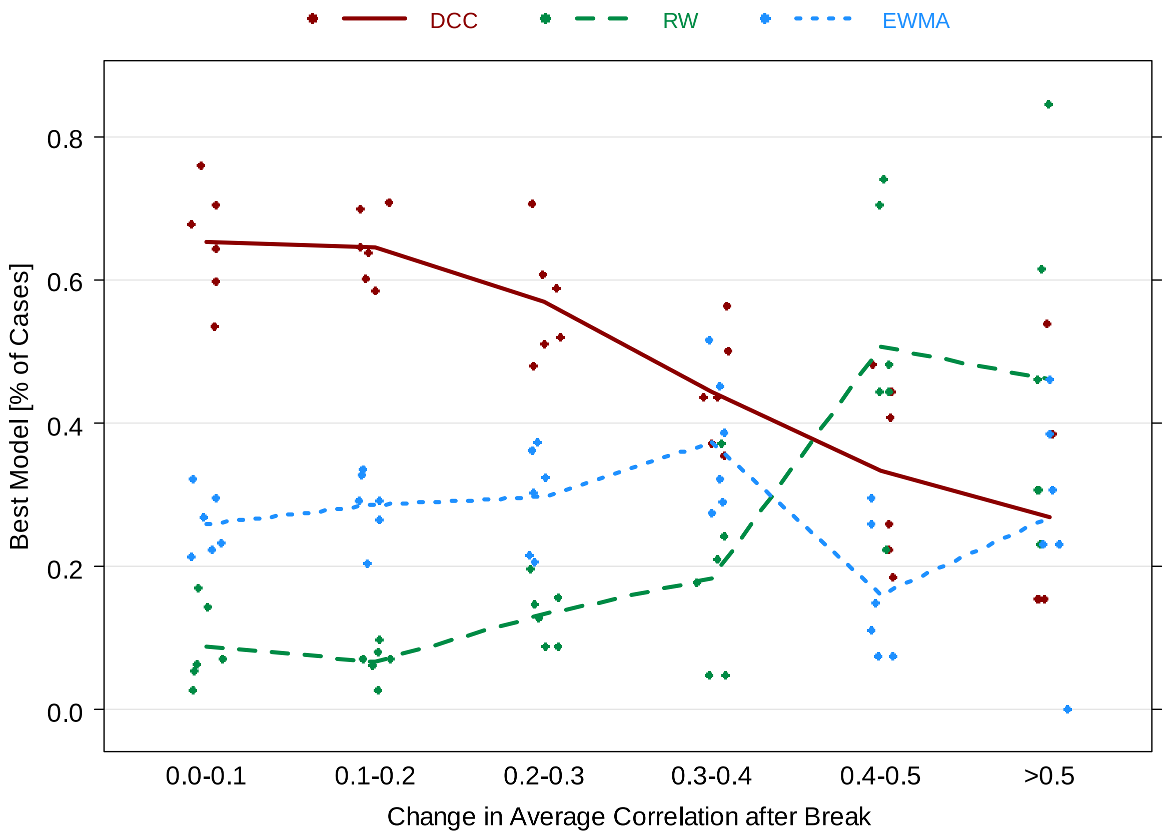

This figure shows the relative performance of asset portfolios based on different dynamic covariance matrix estimators. Panel A shows how break and non-breaks samples with equal size are selected. Panel B shows that the DCC model performs less well in samples containing a correlation break. Panel C shows that when correlation breaks are large, a simple rolling window estimator is the best choice.